

# TIPO: Text to Image with Text Presampling for Prompt Optimization

Shih-Ying Yeh <sup>♣</sup>  
kohaku@kblueleaf.net

Sang-Hyun Park <sup>♡◇</sup>  
angel4th@yonsei.ac.kr

YI LI <sup>♣</sup>  
liyi0067@e.ntu.edu.sg

Giyeong Oh <sup>♡</sup>  
hard2251@yonsei.ac.kr

Xuehai Wang <sup>★</sup>  
lankeqing3910@gmail.com

Min Song <sup>♡◇</sup>  
min.song@yonsei.ac.kr

Youngjae Yu <sup>♡</sup>  
yjy@yonsei.ac.kr

<sup>♣</sup>National Tsing Hua University <sup>♡</sup>Yonsei University <sup>◇</sup>Onoma AI  
<sup>♣</sup>Nanyang Technological University <sup>★</sup>Anhui Medical University

Code: <https://github.com/KohakuBlueleaf/KGen>

## Abstract

*TIPO (Text-to-Image Prompt Optimization) introduces an efficient approach for automatic prompt refinement in text-to-image (T2I) generation. Starting from simple user prompts, TIPO leverages a lightweight pre-trained model to expand these prompts into richer, detailed versions. Conceptually, TIPO samples refined prompts from a targeted sub-distribution within the broader semantic space, preserving the original intent while significantly improving visual quality, coherence, and detail. Unlike resource-intensive methods based on large language models (LLMs) or reinforcement learning (RL), TIPO provides computational efficiency and scalability, opening new possibilities for effective, automated prompt engineering in T2I tasks.*

*We provide visual results, human preference report to investigate TIPO’s effectiveness. Experimental evaluations on benchmark datasets demonstrate substantial improvements in aesthetic quality, significant reduction of visual artifacts, and enhanced alignment with target distributions along with significant human preference proficiency. These results highlight the importance of targeted prompt engineering in text-to-image tasks and indicate broader opportunities for automated prompt refinement.*

## 1. Introduction

The rapid proliferation of Text-to-Image (T2I) generative models have revolutionized artistic creation [7, 8, 14, 15, 20, 21, 35, 48, 50, 53–55, 57, 59, 60]. These models offer direct control over generative visual

content via *text prompts*. To achieve precise control, modern T2I architectures are often trained on lengthy, detailed text descriptions, which may consist of individual, formatted tags of objects, backgrounds, styles, or complex, integrated paragraphs outlining image content and layout. However, the increasing complexity of prompts also forces users to iteratively refine their inputs, making high-quality T2I artwork accessible only to those with significant prompt engineering expertise.

Recently, efforts have been made to reduce the reliance on human expertise through *prompt optimization*, i.e., expanding and refining a user’s primitive input into a more detailed prompt to enhance generation quality. A straightforward approach is to leverage pre-trained Large Language Models (LLMs) to rewrite prompts in a zero-shot manner [42]. Yet, LLMs are primarily trained on general natural language, such as paragraphs and dialogues, which differ significantly from the structured prompts used for T2I models. This discrepancy often leads to additional effort in crafting LLM prompts and increased misalignment between generated images and intended prompts. A more effective approach is to train LLMs directly on prompt data collected from model users [5, 17]. While promising, this method is inherently constrained by the varying levels of user expertise, often resulting in inconsistent or suboptimal outputs. Recent work [26] trains LLM with reinforcement learning, where aesthetic scores of generated images serve as rewards. However, the reinforcement learning is performed on one specific T2I model with high computational cost, hindering its application to a broader variety of models.

Deviating from existing work, we argue that *the op-*

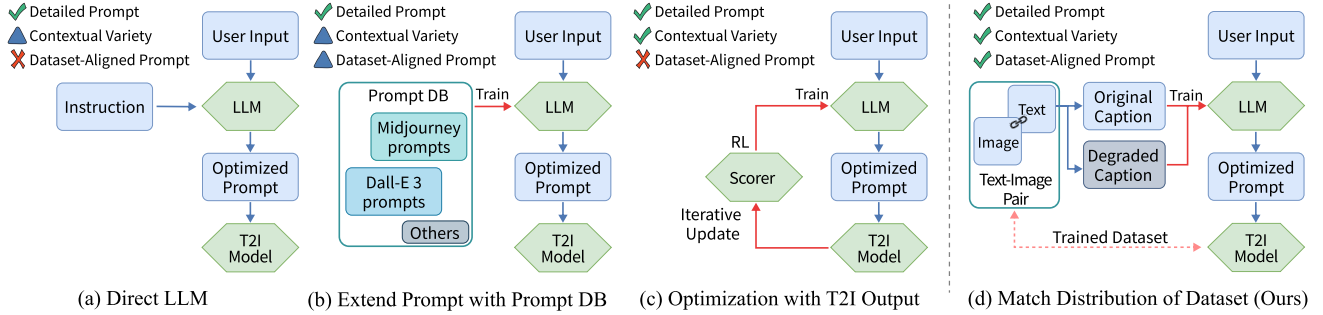


Figure 1. Comparison of prompt optimization methods using LLM. **(a)** uses instructions for prompting but its understanding is constrained by the LLM’s knowledge base, not T2I model. **(b)** relies on a curated prompt database, enhancing detail but limiting variety by not fully leveraging the T2I model’s learned distribution. **(c)** optimizes using the scorer with RL, requiring multi-turn inference with additional cost. **(d)** aligns prompts with the T2I model’s training distribution, ensuring detailed and various topic-related prompt generation that fits the target T2I model.

*timal prompt lies in T2I models’ training set.* Precisely, when a prompt aligns with the data distribution used for model training, the model can better interpret the prompt, resulting in improved text alignment and higher image quality. Based on this insight, we introduce **TIPO** (**T**ext to **I**mage with text pre-sampling for **P**rompt **O**ptimization), an innovative framework designed to enhance T2I generative models. At its core lies a lightweight language model trained on multiple meticulously designed pretext tasks that transform prompts into tags or sentences from coarse to fine. Leveraging the trained model, TIPO can progressively and seamlessly adapt to various user input types, generating accurate and robust prompts for various T2I models. In addition, our training data is derived from a curated text description dataset comprising over 30 million text-image pair samples and more than 20 billion tokens, ensuring comprehensive coverage of T2I training sets. Extensive experiments on test prompts from in- and out-of-domain demonstrate that TIPO consistently outperforms state-of-the-art methods in fidelity, aesthetics, and text alignment. Detailed analysis shows that TIPO has up to 62.80% win rate in user preference and 25% improvement in runtime efficiency over the second-best baseline. To summarize, our contributions are at least three-fold:

1. We introduce TIPO, a prompt optimization framework that leverages the large-scale text data distributions used in text-to-image (T2I) training.
2. We train a multi-task language model, which adaptively and progressively refines user inputs from either tag-based or natural language prompts into unified formats, enhancing compatibility across a broad spectrum of T2I models.
3. Extensive experiments demonstrate that TIPO achieves superior image quality, strong text align-

ment, higher human preference, and improved runtime efficiency across both in-domain and out-of-domain prompts, highlighting its great potential in real-world applications.

## 2. Related Work

Prompt optimization for T2I models typically leverages language models to refine user inputs. They can be broadly classified into two categories: (1) *Model-specific strategies* that tailor prompts for a particular T2I model, and (2) *Universal strategies* that aim to improve prompt quality across a variety of T2I models.

### 2.1. Model-specific Strategies

T2I models generate images whose quality is often measured using metrics such as fidelity, aesthetics, and user preference. These metrics facilitate reinforcement learning approaches that optimize prompts for a specific T2I model. For instance, Promptist [26] fine-tunes a pre-trained language model by using CLIP relevance scores as rewards. Similarly, PAE [44] extends this approach by generating dense text embeddings rather than discrete text tokens, with additional control vectors during online reinforcement learning. However, these methods are computationally intensive, often struggling with a larger number of training prompts. Moreover, a model optimized for one specific T2I system may not generalize well to others. In contrast, our method leverages over 30 million text descriptions to cover a wide range of high-quality prompts, ensuring compatibility with a broad spectrum of T2I models.

### 2.2. Universal Strategies

To reduce the dependency on specific T2I models, some researchers have focused on refining prompts solely using language models. For example, CogView3 [71] em-

ploy GLM-4 [24], and Lee et al. [33] employ GPT-J and Text Style Transfer (TST) techniques, respectively, for prompt enhancement. However, both of them rely heavily on the LLM’s inherent understanding of visual content descriptions, which may result in a misalignment with the diverse requirements of various T2I models. Alternatively, other approaches collect high-quality prompts from T2I model users to fine-tune or train LLMs [5, 17, 63]. Such methods, however, are limited by the inconsistent expertise of users. Conversely, our approach constructs both tag-based and natural language prompts using a large-scale dataset of image-text descriptions, thereby aligning closely with the text distributions underlying T2I models.

### 3. Preliminaries

**Notations.** We present the notations in our work:

- $\mathcal{P}$ : The space of all possible prompts.
- $\mathcal{I}$ : The space of all possible images.
- $p$ : User-provided prompt.
- $p_o$ : Optimized prompt.
- $p_{ps}$ : Sampled modified prompt derived from  $p$ .
- $\mathcal{M}$ : Metadata (e.g., style tags) aiding prompt transformation.
- $\mathcal{T}$ : Transformation function for pre-sampling (e.g., Random augmentation, TIPO or LLM)
- $T_p, T_{ps}$ : Sets of tags for original and pre-sampled prompts.
- $S_p, S_{ps}$ : Ordered lists of natural language descriptions for original and pre-sampled prompts.

**Text-to-Image Model.** A *text-to-image (T2I) model* is a mapping function

$$f(p) \rightarrow \mathcal{I}_p \subseteq \mathcal{I},$$

which maps a user-provided text prompt  $p$  to a subset of images  $\mathcal{I}_p$  corresponding to the prompt.

**Problem statement.** Let  $\mathcal{I}_u$  denote the user’s *intended distribution* over images. The task of *Prompt optimization* is to generate a prompt  $p_o$  that minimizes a distance  $d$  between the T2I output distribution  $\mathcal{I}_p$  and  $\mathcal{I}_u$ :

$$p_o = \arg \min_{p \in \mathcal{P}} d(\mathcal{I}_p, \mathcal{I}_u),$$

where  $d$  is a suitable metric (e.g., Frechet Inception Distance) comparing two image distributions.

### 4. Methodology

We aim to optimize user prompts to enhance image generation quality. Instead of end-to-end optimizations tailored to a single T2I model, our focus is on prompt rewriting that generalizes across a broad spectrum of models. Our core intuition is that an ideal

prompt should align with the texts used in T2I model training. However, rapid advances in image captioning have rendered these texts increasingly diverse and complex. To address this, we propose to (1) design a clearly structured prompt schema compatible with most text descriptions, and (2) implement a pre-sampling algorithm that progressively refines arbitrary, coarse user input into organized, fine-grained prompts.

#### 4.1. Text Set Preparation

Although the text descriptions used for T2I model training are notably diverse, most are image captions that fall into two broad categories: tag-based and natural language (NL)-based captions. Tag-based captions, such as those in the Danbooru2023 dataset [46, 68], use comma-separated, succinct terms to describe image content. In contrast, NL-based captions, typically generated by language models with visual capabilities [1, 2, 6, 16, 18, 34, 37, 67], may comprise multiple sentences. We represent both types using a unified text set  $T = \{t_1, t_2, t_3, \dots, t_n\}$ , where each element is an individual tag or sentence.

While the original image captions are fine-grained and detailed, which can yield high-quality images when all elements are used, they often result in prompts that are excessively lengthy or overloaded with information. Such prompts diverge from typical user input and pose alignment challenges. To mitigate this, we construct a simpler subset  $T_s \subset T$  by removing some tags and sentences from the original set<sup>1</sup>, as detailed in Section 4.2.

#### 4.2. Formatted Prompt Construction

We aim to construct prompts in a unified format compatible with existing image captions. First, we incorporate the common *metadata* present in these image captions, typically represented as `<Category>: <Content>`. These metadata categories primarily include `artist`, `copyright`, `aspect ratio`, `quality`, and `year` (e.g., `quality: masterpiece, artist: Picasso`). This structured metadata is intuitive for users to read and edit, while also providing strong guidance to downstream T2I models on the generation scope.

Next, we construct both tag-based and NL-based prompts using text sets  $T$ . Our design generates both simple (incomplete) and complete prompts for each image, and we train an auto-regressive language model to extend the simple prompts into complete versions. For tag-based prompts, since the tags are largely order-insensitive (i.e., the order has minimal impact on T2I outcomes), we propose a prefix-based dropout strategy.

<sup>1</sup>For long sentences, off-the-shelf text splitters (e.g., FastText) are used to segment them into multiple sentences.

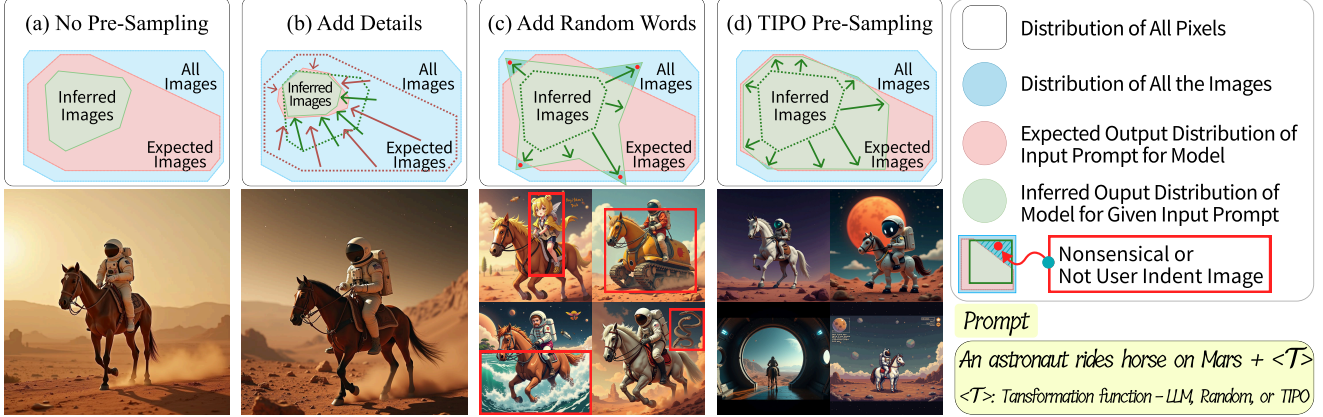


Figure 2. Illustration of various pre-sampling method for generating the T2I prompt `An astronaut rides horse on Mars + <T>`. (a) yields a basic image. (b) enhances details of images but requires manual refinement. (c) adding random words may introduce irrelevant content (red boxes), exceeding the user’s intent. (d) TIPO pre-sampling (ours) aligns outputs with expected intent, maintaining both detail and variety. `<T>` represents a transformation function for pre-sampling.

We first randomly shuffle the complete set of tags  $T = \{t_1, t_2, t_3, \dots, t_n\}$  from a given image caption. Then, we construct a simple tag set  $T_s = \{t_1, t_2, \dots, t_m\}$  by randomly selecting  $m < n$  tags. The prompts are constructed as:

$$p_s = \text{concat}(T_s), \quad p_o = \text{concat}(T)$$

Because  $p_s$  is always a prefix of  $p_o$ , the language model can readily expand the simple tag-based prompt into its complete version.

For NL-based prompts, however, this strategy cannot be applied directly because the first sentence often contains crucial information [25] and the order of sentences significantly influences the caption’s semantics. Therefore, we preserve the first sentence and randomly drop some of the subsequent sentences without changing their order. Let:

$$S = [\text{sentence}_1, \text{sentence}_2, \text{sentence}_3, \dots, \text{sentence}_n]$$

represent the ordered sequence of sentences in an image caption. We derive a simple subsequence  $S_s$  by randomly selecting  $m$  sentences from  $S$  while ensuring that the first sentence is always included and that the original order is maintained. In other words,

$$S_s = [\text{sentence}_{i_1}, \text{sentence}_{i_2}, \dots, \text{sentence}_{i_m}],$$

with  $1 < i_2 < \dots < i_m \leq n$  and  $m < n$ . The simple and complete NL-based prompts are then constructed as:

$$p_s = \text{concat}(S_s), \quad p_o = \text{concat}(S_s, S)$$

This ensures that  $p_s$  remains a prefix of  $p_o$ . Although some sentences may be repeated in  $p_o$ , selecting a smaller  $m$  effectively mitigates this, and it does not empirically affect the generation quality.

### 4.3. Text Pre-sampling

We aim to align user input with the constructed high-quality training prompts  $p_o$  via *pre-sampling*, which stands for “text sampling before image sampling” - a process that first constrains the target distribution in text space before proceeding to image generation. Conceptually, while pre-sampling strategies generally add more text tokens to user input, the outcomes of different strategies may still vary (as illustrated in Figure 2).

To enrich the image content while mitigating undesired output, we perform pre-sampling based on a language model trained on  $p_o$ . A straightforward pre-sampling strategy is to do text completion, i.e., directly append output tokens to the end of user input. However, we posit that *the user input is unlikely to be a part of a good prompt*. The naïve text-completion strategy prioritizes the user’s original input, resulting in worse outcomes as evidenced by Section 5.6.

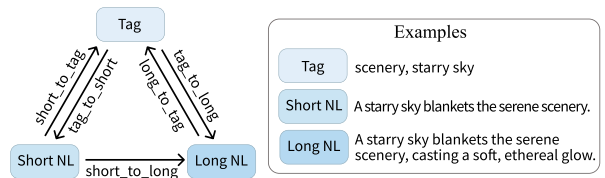


Figure 3. TIPO’s task flow within a single generation. Starting from any node, each arrow represents a sequential extension step, with other prompts used as metadata if provided. This task design enables efficient and flexible prompt extension across multiple tasks.

We propose the core technique of TIPO, a flexible pre-sampling mechanism that divides the prompt op-

timization process into three interconnected subtasks: enriching tag sequences, extending NL prompts, and refining NL prompts. As shown in Figure 3, TIPO uses both tag and NL prompts interchangeably as input sources to generate detailed outputs in various forms. For instance, TIPO can begin with a short NL prompt to produce a detailed tag sequence, denoted as `short_to_tag`. Training data for the language model is constructed by concatenating different types of  $p_o$  with task-specific metadata embedded into the text.

The individual tasks are defined as follows:

- `tag_to_long`: Use tags as metadata to generate a new NL prompt.
- `long_to_tag`: Use an NL prompt as metadata to extend a tag sequence.
- `short_to_tag`: Use the simple prompt  $p_s$  as metadata to extend a tag sequence.
- `short_to_long`: Use a user-provided NL prompt as metadata to generate a refined, detailed prompt.

We also consider composite tasks that can be performed within a single forward pass. These tasks offer the language model a holistic view of the objective while reducing computational overhead:

- `short_to_tag_to_long`: Use a user-provided NL prompt or tag sequence as metadata to generate a refined, detailed prompt.
- `short_to_long_to_tag`: Use a user-provided NL prompt or generated NL prompt as metadata to extend a tag sequence.
- `tag_to_short_to_long`: Use user-provided tags or NL prompts as metadata to generate a refined NL prompt.

We randomly select from the aforementioned tasks during training to enhance model generalization. By extensively training on these tasks, TIPO can seamlessly adapt to various input types, flexibly refining user input whether it consists of tags, short sentences, or long sentences. Figure 4 illustrates a scenario where both tag captions  $T_s$  and short NL captions  $S_s$  are available. In such cases, TIPO processes each input type separately to maintain clarity and coherence:

$$S_s = \{A\text{ young girl with long hair...}\}, \quad \text{metadata} = \emptyset$$

$$T_s = \{\text{outdoors, scenery, water, wind, landscape, ...}\}$$

The generation proceeds sequentially as follows:

1. `short_to_tag`: TIPO uses  $T_s$  as the primary prompt to generate a detailed tag sequence  $T_d$ .
2. `tag_to_long`:  $T_d$  is incorporated into the metadata, and TIPO produces a refined short NL prompt  $S_s$  based on  $T_d$ .

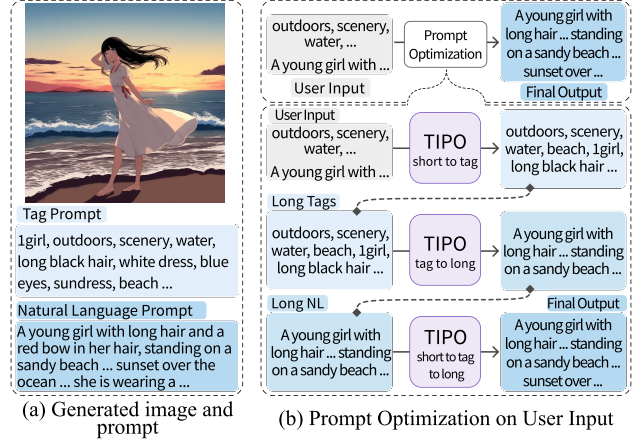


Figure 4. An example scenario of TIPO workflow. (a) A generated image and prompts. (b) Prompt optimization of TIPO, from simple user input  $p_s$  to detailed final output  $p_d$ . The shading from gray to light sky blue represents an increase in context richness in the prompt.

3. `short_to_tag_to_long`: With both  $T_d$  and  $S_s$  in the metadata, TIPO generates a comprehensive long NL prompt  $S_d$ , ensuring a more detailed output.
4. TIPO aggregates  $T_d$ ,  $S_d$ , and any additional metadata to construct a context-rich prompt  $p_d$ .

This progressive process enables TIPO to build prompts that are both detailed and contextually aligned with the user’s input.

#### 4.4. Implementation Details

TIPO can utilize various types of causal autoregressive language models by design. In practice, we leverage the LLaMA architecture [3, 64, 65] for simplicity, with 200M and 500M parameters.

- **TIPO-200M**: Pretrained on the Danbooru2023 [46, 69] and GBC10M [29] datasets for 5 epochs, then fine-tuned with Danbooru2023, GBC10M, and CoyoHD11M [12] for 3 epochs, covering approximately 40 billion tokens.
- **TIPO-500M**: Pretrained on the Danbooru2023, GBC10M, and CoyoHD11M datasets for 5 epochs, covering approximately 30 billion tokens.

## 5. Experiments

### 5.1. Experimental Settings

**Baselines.** We compare with state-of-the-art prompt optimization methods as follows:

- GPT [2] series are powerful large language models capable of zero-shot prompt optimization. We use GPT-4o-mini for lower cost and better efficiency.

- MagicPrompt [17] trains GPT-2 on high-quality prompts collected from stable-diffusion model users.
- Promptist [26] optimizes user input into model-preferred prompts via reinforcement learning.

**Evaluation Metrics.** We employ four latest metrics FDD [61], Aesthetic Score [19], AI Corrupt Score [45], and Vendi Score [22] to measure the quality of generated images. Specifically, FDD (Frechet Dino Distance) measures the image fidelity using the similarity between generated and dataset images via DinoV2 features [47], which better aligns with human perception than traditional FID [28]. Aesthetic Score is computed via Aesthetic Predictor V2.5 [19], quantifying visual appeal, composition quality, and artistic merit. AI Corrupt Score detects technical flaws in generated images by identifying visual artifacts. Vendi Score quantifies image diversity by calculating the von Neumann entropy from a normalized cosine similarity matrix using DinoV2 embeddings.

**Evaluation Protocols.** Our proposed TIPO leverages large-scale image caption datasets for training, which overlap with the training text distributions of many T2I models. Following Promptist [26], we divide our experiments into two settings: (1) **In-domain**, where the T2I model’s training texts overlap with those used by TIPO, and (2) **Out-of-domain**, where no overlap exists.

## 5.2. In-domain Tag-based Prompt Optimization

To assess prompt optimization performance on tag-based prompts, we generate scenery images, as they contain abundant descriptive tags for objects and backgrounds. We randomly sample 32,768 tag-based prompts from Danbooru2023 [46, 69], shuffle and concatenate the scenery tags into new prompts (thereby preventing data leakage of the original captions), and generate one image per prompt using Kohaku-XL-Zeta, an SDXL [46, 50] variant fine-tuned on Danbooru2023. This evaluation tests the *in-domain* capabilities, as Danbooru2023 is also used during TIPO training.

Metric	Original	GPT	MagicPrompt	Promptist	TIPO (Ours)
FDD ↓	0.3558	0.5414	0.3247	<u>0.2350</u>	<b>0.2282</b>
Aesthetic Score ↑	5.0569	<b>6.3676</b>	6.1609	5.9468	<u>6.2571</u>
AI Corrupt Score ↑	0.4257	<u>0.7490</u>	0.5024	0.5669	<b>0.9195</b>
Vendi Score ↑	<b>16.8135</b>	8.6632	11.9014	<u>14.3273</u>	13.3070

Table 1. Performance on in-domain tag-based prompts, with best results bolded and the second-best underlined.

The results in Table 1 reveal two key insights. First, MagicPrompt and Promptist, which rely on user prompts or reinforcement learning, underperform in Aesthetic and AI Corrupted Scores due to the quality

or quantity limitations of their collected samples (e.g., Promptist uses 90K samples, limited by the high reinforcement learning cost). In contrast, GPT and TIPO benefit from large-scale training corpora (>30M samples), yielding higher-quality outputs. Second, TIPO achieves the best FDD by a substantial margin over GPT, which can be attributed to its superior distribution alignment with T2I models.

## 5.3. In-domain NL-based Prompt Optimization

We evaluate the prompt optimization performance on NL-based prompts by selecting 10,000 short prompts and 10,000 long prompts from CaptionEmporium [12] and GBC [29] as test prompts. In particular, since the long prompts are much longer than typical user input, we truncate them to two sentences (< 40 words) to simulate real-world applications. We use SDXL-1.0-base [50] as the T2I model, whose training text data largely overlap with TIPO.

Short	Original	GPT	MagicPrompt	Promptist	TIPO(Ours)
FDD ↓	<b>0.0957</b>	0.1668	<u>0.0980</u>	0.1783	0.1168
Aesthetic Score ↑	5.8370	<b>6.0589</b>	5.8213	5.7963	<u>5.8531</u>
AI Corrupt Score ↑	<u>0.7113</u>	0.6985	0.7064	0.6314	<b>0.7131</b>
Vendi Score ↑	<b>38.1715</b>	34.7139	<u>38.1553</u>	34.1270	37.0649
Truncated Long	Original	GPT	MagicPrompt	Promptist	TIPO(Ours)
FDD ↓	<b>0.0955</b>	0.1683	0.1247	0.2096	<u>0.1210</u>
Aesthetic Score ↑	5.7497	<b>6.0168</b>	5.8191	5.7759	<u>5.8364</u>
AI Corrupt Score ↑	<u>0.6868</u>	0.6712	0.6741	0.5925	<b>0.7130</b>
Vendi Score ↑	<b>38.2533</b>	34.8108	<u>37.8412</u>	33.5266	37.0900

Table 2. Performance on in-domain NL-based prompts.

Table 2 demonstrates that TIPO achieves either the best or second-best scores in Aesthetic and AI Corrupt Score by effectively enriching the original prompt with appropriate textual elements while rarely introducing extraneous noise. While all methods compromise fidelity and diversity, as reflected in the FDD and Vendi Score, TIPO remains competitive because it maintains small semantic deviation from the original sentences via progressive refinement.

## 5.4. Out-of-domain Performance

Some recent T2I models are trained on proprietary images and captions. As a representative example, SD-3.5-Large[20] is trained on private images captioned with CogView[71], which differ markedly from the texts used to train TIPO. To evaluate model performance in this out-of-domain scenario, we generate 8,192 original tag- and NL-based prompts using the baseline GPT-4o-mini rather than relying on existing prompt datasets. We apply the remaining methods to these prompts and assess their performance.

As shown in Table 3, SD-3.5-Large faithfully generates images that align well with GPT-produced

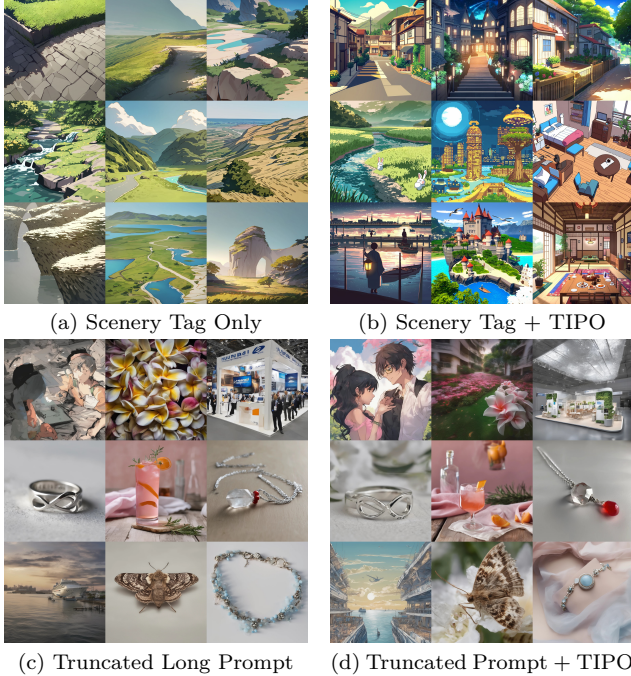


Figure 5. Generated images from 4 types of prompts: (a) simple scenery tag, (b) scenery tag enhanced by TIPO, (c) truncated (< 40 words) long prompt, (d) TIPO-enhanced truncated prompt. TIPO adds detail and maintains variety, yielding coherent images from simple prompts.

	GPT	MagicPrompt	Promptist	TIPO(Ours)
Aesthetic Score ↑	<b>6.7125</b>	<u>6.4507</u>	6.3924	6.0536
AI Corrupt Score ↑	<b>0.9482</b>	0.8577	0.9053	<u>0.9280</u>
Vendi Score ↑	8.9718	15.8721	<u>16.4891</u>	<b>21.5706</b>

Table 3. Performance on the out-of-domain T2I model

prompts. Consequently, additional optimizations tend to reduce fidelity and introduce more artifacts. Nevertheless, GPT-generated prompts are accurate and lack diversity. TIPO optimization enriches the prompts with additional details that harmonize with the original themes, significantly enhancing the diversity of the generated images.

### 5.5. Human Preference Evaluation

Quantitative metrics may not fully align with human preference. Therefore, we conducted a user study based on pairwise image comparisons between the original prompt, MagicPrompt, Promptist, and TIPO on over 1,400 images, gathering preferences from 221 volunteers. As illustrated in Figure 7, TIPO achieved the highest overall win rate at 51.3%, significantly outperforming competitors. In out-of-domain scenarios, TIPO’s win rate increased to 52.5%, demonstrating

consistently strong user preference across different contexts. For further results and statistics, please refer to Appendix F.

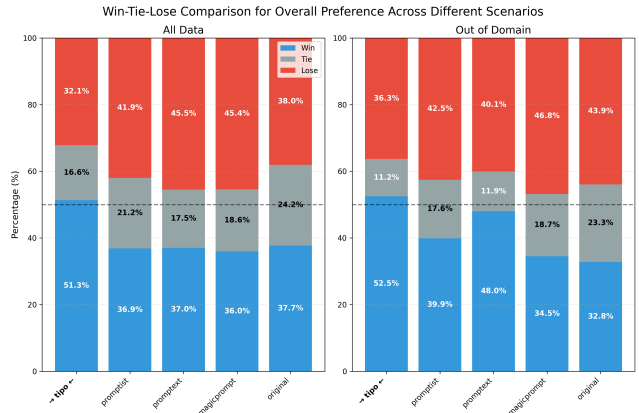


Figure 7. The win-tie-lose rate on overall preference on all data and out-of-domain situation where images are generated by SD-3.5-Medium.

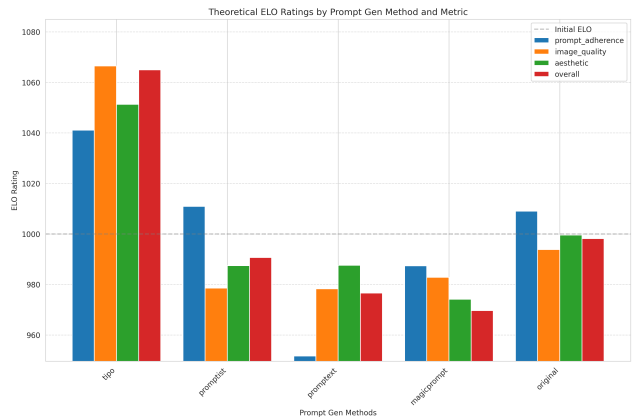


Figure 8. ELO rating on overall preference on all data

### 5.6. Ablation Study

	Original	Completion	TIPO
Aesthetic Score ↑	5.9507	<u>5.9631</u>	<b>5.9960</b>
Corrupt Score ↑	0.6799	<u>0.8131</u>	<b>0.8971</b>
Vendi Score ↑	<b>19.7208</b>	<u>18.2896</u>	13.9864

Table 4. Ablation results

We attribute TIPO’s success primarily to its multi-task pre-sampling design detailed in Section 4.3. However, a natural question arises: can a simple text completion approach achieve similar or better results? To validate



Figure 6. Qualitative comparison of prompt completion versus TIPO (ours). (a) shows images generated by original prompts. (b) depicts images generated by text completion using **TIPO-500M**. (c) shows images generated by TIPO.

our design, we compare TIPO’s pre-sampling strategy with a direct text completion using the same language model, **TIPO-500M**. As shown in Table 4, TIPO significantly improves aesthetic scores and reduces artifacts compared to text completion. For visual examples, please refer to Figure 6. For more ablation details and visualization, please refer to Appendix 5.6.

## 6. Conclusion

We introduced TIPO, a lightweight prompt pre-sampling framework designed for efficient real-world Text-to-Image (T2I) applications. By aligning user prompts with the intrinsic distributions of T2I training datasets, TIPO enhances semantic coherence, image fidelity, and diversity with minimal inference overhead.

TIPO consistently outperforms existing prompt optimization methods, achieving superior performance across multiple evaluation metrics. Its ability to preserve user intent while enhancing prompt diversity and image quality makes it well-suited for both in-domain and out-of-domain scenarios, demonstrating robustness across various prompt formats and model architectures.

Extensive user studies also confirmed TIPO’s strong alignment with human preferences, further highlighting its potential for practical applications. To encourage wider adoption and facilitate reproducibility, we release our trained models and source code. We hope TIPO will inspire further advancements in efficient, scalable, and robust generative frameworks for creative systems.

## References

- [1] Pravesh Agrawal, Szymon Antoniak, Emma Bou Hanna, Baptiste Bout, Devendra Chaplot, Jessica Chudnovsky, Diogo Costa, Baudouin De Monicault, Saurabh Garg, Theophile Gervet, Soham Ghosh, Amélie Héliou, Paul Jacob, Albert Q. Jiang, Kartik Khandelwal, Timothée Lacroix, Guillaume Lample, Diego Las Casas, Thibaut Lavril, Teven Le Scao, Andy Lo, William Marshall, Louis Martin, Arthur Mensch, Pavankumar Muddireddy, Valera Nemychnikova, Marie Pellat, Patrick Von Platen, Nikhil Raghuraman, Baptiste Rozière, Alexandre Sablayrolles, Lucile Saulnier, Romain Sauvestre, Wendy Shang, Roman Soletskyi, Lawrence Stewart, Pierre Stock, Joachim Studnia, Sandeep Subramanian, Sagar Vaze, Thomas Wang, and Sophia Yang. Pixtral 12b, 2024. 3, 15
- [2] Open AI. Hello gpt-4o, 2024. 3, 5
- [3] AI@Meta. Llama 3 model card. 2024. 5, 13
- [4] Michael S Albergo and Eric Vanden-Eijnden. Building normalizing flows with stochastic interpolants. *arXiv preprint arXiv:2209.15571*, 2022. 14
- [5] AUTOMATIC. promptgen-lexart. <https://huggingface.co/AUTOMATIC/promptgen-lexart>, 2022. 1, 3
- [6] Jinze Bai, Shuai Bai, Shusheng Yang, Shijie Wang, Sinan Tan, Peng Wang, Junyang Lin, Chang Zhou, and Jingren Zhou. Qwen-vl: A frontier large vision-language model with versatile abilities. *arXiv preprint arXiv:2308.12966*, 2023. 3
- [7] James Betker, Gabriel Goh, Li Jing, Tim Brooks, Jianfeng Wang, Linjie Li, Long Ouyang, Juntang

- Zhuang, Joyce Lee, Yufei Guo, et al. Improving image generation with better captions. *Computer Science*. <https://cdn.openai.com/papers/dall-e-3.pdf>, 2(3):8, 2023. 1
- [8] black-forest labs. black-forest-labs/flux: Official inference repo for FLUX.1 models. <https://github.com/black-forest-labs/flux>, 2024. 1
- [9] David M Blei, Andrew Y Ng, and Michael I Jordan. Latent dirichlet allocation. *Journal of machine Learning research*, 3(Jan):993–1022, 2003. 39
- [10] Vincent D Blondel, Jean-Loup Guillaume, Renaud Lambiotte, and Etienne Lefebvre. Fast unfolding of communities in large networks. *Journal of Statistical Mechanics: Theory and Experiment*, 2008(10):P10008, 2008. 40
- [11] Phillip Bonacich. Factoring and weighting approaches to status scores and clique identification. *Journal of Mathematical Sociology*, 2(1):113–120, 1972. 40
- [12] CaptionEmporium. CaptionEmporium/coyo-hd-11m-llavanext. <https://huggingface.co/datasets/CaptionEmporium/coyo-hd-11m-llavanext>, 2024. 5, 6, 13, 15
- [13] Soravit Changpinyo, Piyush Sharma, Nan Ding, and Radu Soricut. Conceptual 12M: Pushing web-scale image-text pre-training to recognize long-tail visual concepts. In *CVPR*, 2021. 13
- [14] Junsong Chen, Chongjian Ge, Enze Xie, Yue Wu, Lewei Yao, Xiaozhe Ren, Zhongdao Wang, Ping Luo, Huchuan Lu, and Zhenguo Li. Pixart- $\Sigma$ : Weak-to-strong training of diffusion transformer for 4k text-to-image generation, 2024. 1
- [15] Junsong Chen, Jincheng YU, Chongjian GE, Lewei Yao, Enze Xie, Zhongdao Wang, James Kwok, Ping Luo, Huchuan Lu, and Zhenguo Li. Pixart- $\alpha$ : Fast training of diffusion transformer for photorealistic text-to-image synthesis. In *The Twelfth International Conference on Learning Representations*, 2024. 1
- [16] Wenliang Dai, Nayeon Lee, Boxin Wang, Zhuoling Yang, Zihan Liu, Jon Barker, Tuomas Rintamaki, Mohammad Shoeybi, Bryan Catanzaro, and Wei Ping. Nvlm: Open frontier-class multimodal llms. *arXiv preprint arXiv:2409.11402*, 2024. 3
- [17] daspartho. prompt-extend. <https://huggingface.co/daspartho/prompt-extend>, 2022. 1, 3, 6
- [18] Matt Deitke, Christopher Clark, Sangho Lee, Rohun Tripathi, Yue Yang, Jae Sung Park, Mohammadreza Salehi, Niklas Muennighoff, Kyle Lo, Luca Soldaini, et al. Molmo and pixmo: Open weights and open data for state-of-the-art multimodal models. *arXiv preprint arXiv:2409.17146*, 2024. 3
- [19] discuss0434. aesthetic-predictor-v2-5: SigLIP-based Aesthetic Score Predictor. <https://github.com/discuss0434/aesthetic-predictor-v2-5>, 2024. 6
- [20] Patrick Esser, Sumith Kulal, Andreas Blattmann, Rahim Entezari, Jonas Müller, Harry Saini, Yam Levi, Dominik Lorenz, Axel Sauer, Frederic Boesel, et al. Scaling rectified flow transformers for high-resolution image synthesis. In *Forty-first International Conference on Machine Learning*, 2024. 1, 6, 14
- [21] Patrick Esser, Sumith Kulal, Andreas Blattmann, Rahim Entezari, Jonas Müller, Harry Saini, Yam Levi, Dominik Lorenz, Axel Sauer, Frederic Boesel, Dustin Podell, Tim Dockhorn, Zion English, Kyle Lacey, Alex Goodwin, Yannik Marek, and Robin Rombach. Scaling rectified flow transformers for high-resolution image synthesis, 2024. 1, 22
- [22] Dan Friedman and Adji Bousso Dieng. The vendi score: A diversity evaluation metric for machine learning. *arXiv preprint arXiv:2210.02410*, 2022. 6
- [23] Georgi Gerganov. GitHub - ggerganov/llama.cpp: LLM inference in C/C++ — github.com. <https://github.com/ggerganov/llama.cpp>, 2023. 16
- [24] Team GLM, :, Aohan Zeng, Bin Xu, Bowen Wang, Chenhui Zhang, Da Yin, Dan Zhang, Diego Rojas, Guanyu Feng, Hanlin Zhao, Hanyu Lai, Hao Yu, Hongning Wang, Jiadai Sun, Jiajie Zhang, Jiale Cheng, Jiayi Gui, Jie Tang, Jing Zhang, Jingyu Sun, Juanzi Li, Lei Zhao, Lindong Wu, Lucien Zhong, Mingdao Liu, Minlie Huang, Peng Zhang, Qinkai Zheng, Rui Lu, Shuaiqi Duan, Shudan Zhang, Shulin Cao, Shuxun Yang, Weng Lam Tam, Wenyi Zhao, Xiao Liu, Xiao Xia, Xiaohan Zhang, Xiaotao Gu, Xin Lv, Xinghan Liu, Xinyi Liu, Xinyue Yang, Xixuan Song, Xunkai Zhang, Yifan An, Yifan Xu, Yilin Niu, Yuan-tao Yang, Yueyan Li, Yushi Bai, Yuxiao Dong, Zehan Qi, Zhaoyu Wang, Zhen Yang, Zhengxiao Du, Zhenyu Hou, and Zihan Wang. Chatglm: A family of large language models from glm-130b to glm-4 all tools, 2024. 3
- [25] Aditi Godbole, Jabin Geevarghese George, and Smita Shandilya. Leveraging long-context large language models for multi-document understanding and summarization in enterprise applications, 2024. 4
- [26] Yaru Hao, Zewen Chi, Li Dong, and Furu Wei. Optimizing prompts for text-to-image generation. In *Thirty-seventh Conference on Neural Information Processing Systems*, 2023. 1, 2, 6
- [27] John A Hartigan, Manchek A Wong, et al. A k-means clustering algorithm. *Applied statistics*, 28(1):100–108, 1979. 39
- [28] Martin Heusel, Hubert Ramsauer, Thomas Unterthiner, Bernhard Nessler, and Sepp Hochreiter. Gans trained by a two time-scale update rule converge to a local nash equilibrium. In *Advances in Neural Information Processing Systems*. Curran Associates, Inc., 2017. 6
- [29] Yu-Guan Hsieh, Cheng-Yu Hsieh, Shih-Ying Yeh, Louis Béthune, Hadi Pour Ansari, Pavan Kumar Anasosalu Vasu, Chun-Liang Li, Ranjay Krishna, Oncel Tuzel, and Marco Cuturi. Graph-based captioning: Enhancing visual descriptions by interconnecting region captions, 2024. 5, 6, 13, 15
- [30] Edward J Hu, Yelong Shen, Phillip Wallis, Zeyuan Allen-Zhu, Yuanzhi Li, Shean Wang, Lu Wang, Weizhu

- Chen, et al. Lora: Low-rank adaptation of large language models. *ICLR*, 1(2):3, 2022. 41
- [31] Gabriel Ilharco, Mitchell Wortsman, Ross Wightman, Cade Gordon, Nicholas Carlini, Rohan Taori, Achal Dave, Vaishaal Shankar, Hongseok Namkoong, John Miller, Hannaneh Hajishirzi, Ali Farhadi, and Ludwig Schmidt. Openclip, 2021. If you use this software, please cite it as below. 13
- [32] Hamed Jelodar, Yongli Wang, Chi Yuan, Xia Feng, Xiahui Jiang, Yanchao Li, and Liang Zhao. Latent dirichlet allocation (lda) and topic modeling: models, applications, a survey, 2018. 39
- [33] Seunghun Lee, Jihoon Lee, Chan Ho Bae, Myung-Seok Choi, Ryong Lee, and Sangtae Ahn. Optimizing prompts using in-context few-shot learning for text-to-image generative models. *IEEE Access*, 12:2660–2673, 2024. 3
- [34] Bo Li, Yuanhan Zhang, Dong Guo, Renrui Zhang, Feng Li, Hao Zhang, Kaichen Zhang, Yanwei Li, Ziwei Liu, and Chunyuan Li. Llava-onevision: Easy visual task transfer. *arXiv preprint arXiv:2408.03326*, 2024. 3
- [35] Zhimin Li, Jianwei Zhang, Qin Lin, Jiangfeng Xiong, Yanxin Long, Xincheng Deng, Yingfang Zhang, Xingchao Liu, Minbin Huang, Zedong Xiao, Dayou Chen, Jiajun He, Jiahao Li, Wenyue Li, Chen Zhang, Rongwei Quan, Jianxiang Lu, Jiabin Huang, Xiaoyan Yuan, Xiaoxiao Zheng, Yixuan Li, Jihong Zhang, Chao Zhang, Meng Chen, Jie Liu, Zheng Fang, Weiyang Wang, Jinbao Xue, Yangyu Tao, Jianchen Zhu, Kai Liu, Sihuan Lin, Yifu Sun, Yun Li, Dongdong Wang, Mingtao Chen, Zhichao Hu, Xiao Xiao, Yan Chen, Yuhong Liu, Wei Liu, Di Wang, Yong Yang, Jie Jiang, and Qinglin Lu. Hunyuan-dit: A powerful multi-resolution diffusion transformer with fine-grained chinese understanding, 2024. 1
- [36] Yaron Lipman, Ricky TQ Chen, Heli Ben-Hamu, Maximilian Nickel, and Matt Le. Flow matching for generative modeling. *arXiv preprint arXiv:2210.02747*, 2022. 14
- [37] Haotian Liu, Chunyuan Li, Qingyang Wu, and Yong Jae Lee. Visual instruction tuning. In *Advances in Neural Information Processing Systems*, pages 34892–34916. Curran Associates, Inc., 2023. 3
- [38] Haotian Liu, Chunyuan Li, Yuheng Li, Bo Li, Yuanhan Zhang, Sheng Shen, and Yong Jae Lee. Llava-next: Improved reasoning, ocr, and world knowledge, 2024. 13
- [39] Xingchao Liu, Chengyue Gong, and Qiang Liu. Flow straight and fast: Learning to generate and transfer data with rectified flow. *arXiv preprint arXiv:2209.03003*, 2022. 14
- [40] I Loshchilov. Decoupled weight decay regularization. *arXiv preprint arXiv:1711.05101*, 2017. 15
- [41] Ilya Loshchilov and Frank Hutter. SGDR: Stochastic gradient descent with warm restarts. In *International Conference on Learning Representations*, 2017. 15
- [42] Oscar Mañas, Pietro Astolfi, Melissa Hall, Candace Ross, Jack Urbanek, Adina Williams, Aishwarya Agrawal, Adriana Romero-Soriano, and Michal Drozdal. Improving text-to-image consistency via automatic prompt optimization, 2024. 1
- [43] Rada Mihalcea and Paul Tarau. TextRank: Bringing order into text. In *Proceedings of the 2004 Conference on Empirical Methods in Natural Language Processing*, pages 404–411, Barcelona, Spain, 2004. Association for Computational Linguistics. 39
- [44] Wenyi Mo, Tianyu Zhang, Yalong Bai, Bing Su, Ji-Rong Wen, and Qing Yang. Dynamic prompt optimizing for text-to-image generation. In *Proceedings of the IEEE/CVF Conference on Computer Vision and Pattern Recognition*, pages 26627–26636, 2024. 2
- [45] narugo1992. Ai-corrupt score for anime images. [https://huggingface.co/deepghs/ai\\_image\\_corrupted](https://huggingface.co/deepghs/ai_image_corrupted), 2023. 6
- [46] nyanko202. Danbooru2023: A large-scale crowdsourced and tagged anime illustration dataset. <https://huggingface.co/datasets/nyanko7/danbooru2023>, 2023. 3, 5, 6, 13, 15
- [47] Maxime Oquab, Timothée Darcet, Theo Moutakanni, Huy V. Vo, Marc Szafraniec, Vasil Khalidov, Pierre Fernandez, Daniel Haziza, Francisco Massa, Alaaeldin El-Nouby, Russell Howes, Po-Yao Huang, Hu Xu, Vasu Sharma, Shang-Wen Li, Wojciech Galuba, Mike Rabbat, Mido Assran, Nicolas Ballas, Gabriel Synnaeve, Ishan Misra, Herve Jegou, Julien Mairal, Patrick Labatut, Armand Joulin, and Piotr Bojanowski. Dinov2: Learning robust visual features without supervision, 2023. 6
- [48] Juan Ossa, Eren Doğan, Alex Birch, and F Johnson. Improvements to sdxl in novelai diffusion v3. *arXiv preprint arXiv:2409.15997*, 2024. 1
- [49] Sang Hyun Park, Jun Young Koh, Junha Lee, Joy Song, Dongha Kim, Hoyeon Moon, Hyunju Lee, and Min Song. Illustrious: an open advanced illustration model, 2024. 37
- [50] Dustin Podell, Zion English, Kyle Lacey, Andreas Blattmann, Tim Dockhorn, Jonas Müller, Joe Penna, and Robin Rombach. SDXL: Improving latent diffusion models for high-resolution image synthesis. In *The Twelfth International Conference on Learning Representations*, 2024. 1, 6, 13
- [51] Alec Radford, Jong Wook Kim, Chris Hallacy, Aditya Ramesh, Gabriel Goh, Sandhini Agarwal, Girish Sastry, Amanda Askell, Pamela Mishkin, Jack Clark, et al. Learning transferable visual models from natural language supervision. In *International conference on machine learning*, pages 8748–8763. PMLR, 2021. 13
- [52] Colin Raffel, Noam Shazeer, Adam Roberts, Katherine Lee, Sharan Narang, Michael Matena, Yanqi Zhou, Wei Li, and Peter J Liu. Exploring the limits of transfer learning with a unified text-to-text transformer. *Journal of machine learning research*, 21(140):1–67, 2020. 14

- [53] Aditya Ramesh, Mikhail Pavlov, Gabriel Goh, Scott Gray, Chelsea Voss, Alec Radford, Mark Chen, and Ilya Sutskever. Zero-shot text-to-image generation. In *Proceedings of the 38th International Conference on Machine Learning*, pages 8821–8831. PMLR, 2021. 1
- [54] Aditya Ramesh, Prafulla Dhariwal, Alex Nichol, Casey Chu, and Mark Chen. Hierarchical text-conditional image generation with clip latents, 2022.
- [55] Robin Rombach, Andreas Blattmann, Dominik Lorenz, Patrick Esser, and Björn Ommer. High-resolution image synthesis with latent diffusion models. In *Proceedings of the IEEE/CVF Conference on Computer Vision and Pattern Recognition (CVPR)*, pages 10684–10695, 2022. 1
- [56] Robin Rombach, Andreas Blattmann, Dominik Lorenz, Patrick Esser, and Björn Ommer. High-resolution image synthesis with latent diffusion models. In *Proceedings of the IEEE/CVF conference on computer vision and pattern recognition*, pages 10684–10695, 2022. 13
- [57] Chitwan Saharia, William Chan, Saurabh Saxena, Lala Li, Jay Whang, Emily L Denton, Kamyar Ghasemipour, Raphael Gontijo Lopes, Burcu Karagol Ayan, Tim Salimans, Jonathan Ho, David J Fleet, and Mohammad Norouzi. Photorealistic text-to-image diffusion models with deep language understanding. In *Advances in Neural Information Processing Systems*, pages 36479–36494. Curran Associates, Inc., 2022. 1
- [58] Tim Salimans and Jonathan Ho. Progressive distillation for fast sampling of diffusion models, 2022. 13
- [59] Axel Sauer, Frederic Boesel, Tim Dockhorn, Andreas Blattmann, Patrick Esser, and Robin Rombach. Fast high-resolution image synthesis with latent adversarial diffusion distillation, 2024. 1
- [60] Zhan Shi, Xu Zhou, Xipeng Qiu, and Xiaodan Zhu. Improving image captioning with better use of captions, 2020. 1
- [61] George Stein, Jesse C. Cresswell, Rasa Hosseinzadeh, Yi Sui, Brendan Leigh Ross, Valentin Vilecroze, Zhaoyan Liu, Anthony L. Caterini, Eric Taylor, and Gabriel Loaiza-Ganem. Exposing flaws of generative model evaluation metrics and their unfair treatment of diffusion models. In *Thirty-seventh Conference on Neural Information Processing Systems*, 2023. 6
- [62] Keith Stevens, Philip Kegelmeyer, David Andrzejewski, and David Buttler. Exploring topic coherence over many models and many topics. In *Proceedings of the 2012 Joint Conference on Empirical Methods in Natural Language Processing and Computational Natural Language Learning*, pages 952–961, Jeju Island, Korea, 2012. Association for Computational Linguistics. 39
- [63] succinctly. text2image-prompt-generator. <https://huggingface.co/succinctly/text2image-prompt-generator>, 2022. 3
- [64] Hugo Touvron, Thibaut Lavril, Gautier Izacard, Xavier Martinet, Marie-Anne Lachaux, Timothée Lacroix, Baptiste Rozière, Naman Goyal, Eric Hambro, Faisal Azhar, Aurelien Rodriguez, Armand Joulin, Edouard Grave, and Guillaume Lample. Llama: Open and efficient foundation language models, 2023. 5
- [65] Hugo Touvron, Louis Martin, Kevin Stone, Peter Albert, Amjad Almahairi, Yasmine Babaei, Nikolay Bashlykov, Soumya Batra, Prajjwal Bhargava, Shrutu Bhosale, Dan Bikel, Lukas Blecher, Cristian Canton Ferrer, Moya Chen, Guillem Cucurull, David Esiobu, Jude Fernandes, Jeremy Fu, Wenyin Fu, Brian Fuller, Cynthia Gao, Vedanuj Goswami, Naman Goyal, Anthony Hartshorn, Saghar Hosseini, Rui Hou, Hakan Inan, Marcin Kardas, Viktor Kerkez, Madian Khabsa, Isabel Kloumann, Artem Korenev, Punit Singh Koura, Marie-Anne Lachaux, Thibaut Lavril, Jenya Lee, Diana Liskovich, Yinghai Lu, Yuning Mao, Xavier Martinet, Todor Mihaylov, Pushkar Mishra, Igor Molybog, Yixin Nie, Andrew Poulton, Jeremy Reizenstein, Rashi Rungta, Kalyan Saladi, Alan Schelten, Ruan Silva, Eric Michael Smith, Ranjan Subramanian, Xiaoqing Ellen Tan, Binh Tang, Ross Taylor, Adina Williams, Jian Xiang Kuan, Puxin Xu, Zheng Yan, Iliyan Zarov, Yuchen Zhang, Angela Fan, Melanie Kambadur, Sharan Narang, Aurelien Rodriguez, Robert Stojnic, Sergey Edunov, and Thomas Scialom. Llama 2: Open foundation and fine-tuned chat models, 2023. 5, 14, 41
- [66] Ashish Vaswani, Noam Shazeer, Niki Parmar, Jakob Uszkoreit, Llion Jones, Aidan N Gomez, Lukasz Kaiser, and Illia Polosukhin. Attention is all you need. *Advances in neural information processing systems*, 30, 2017. 41
- [67] Bin Xiao, Haiping Wu, Weijian Xu, Xiyang Dai, Houdong Hu, Yumao Lu, Michael Zeng, Ce Liu, and Lu Yuan. Florence-2: Advancing a unified representation for a variety of vision tasks. In *Proceedings of the IEEE/CVF Conference on Computer Vision and Pattern Recognition*, pages 4818–4829, 2024. 3
- [68] Shih-Ying Yeh. HakuBooru: text-image dataset maker for anime-style images. <https://github.com/KohakuBlueleaf/HakuBooru>, 2024. 3, 13
- [69] Shih-Ying Yeh. danbooru2023-webp-4Mpixel. <https://huggingface.co/datasets/KBlueLeaf/danbooru2023-webp-4Mpixel>, 2024. 5, 6, 13, 27
- [70] Ying Zhao and George Karypis. Evaluation of hierarchical clustering algorithms for document datasets. In *Proceedings of the Eleventh International Conference on Information and Knowledge Management*, page 515–524, New York, NY, USA, 2002. Association for Computing Machinery. 39
- [71] Wendi Zheng, Jiayan Teng, Zhuoyi Yang, Weihang Wang, Jidong Chen, Xiaotao Gu, Yuxiao Dong, Ming Ding, and Jie Tang. Cogview3: Finer and faster text-to-image generation via relay diffusion, 2024. 2, 6

---

# Appendix

---

## Table of Contents

A. Dataset/Resource	13
A.1. Danbooru2023 . . . . .	13
A.2. GBC10M . . . . .	13
A.3. Coyo HD 11M . . . . .	13
A.4. Stable Diffusion XL . . . . .	13
A.5. Illustrious. . . . .	13
A.6. Stable Diffusion 3.5 . . . . .	14
B. Implementation Details	14
B.1. Training Data Construction . . . . .	14
B.2. Training Settings and Model Configurations . . . . .	14
B.3. Inference Pipeline . . . . .	16
B.4. Model Speed Comparison . . . . .	16
C. Evaluation Statistics	17
C.1. In-domain test regarding scenery tag . . . . .	17
C.2. In-domain prompt generation test . . . . .	18
C.3. Out-of-domain evaluation . . . . .	20
C.4. Ablation Test . . . . .	23
D. TIPO example	25
E. Image Examples	27
E.1. In-domain test regard to scenery tag . . . . .	27
E.2. In-domain prompt generation test . . . . .	27
F. Human Preference	28
F.1. User Interface for Human Preference Evaluation . . . . .	28
F.2. Extended Human Evaluation. . . . .	31
F.3. ELO Ratings. . . . .	31
F.4. Human Preference ELO Method . . . . .	31
F.5. Statistical Significance . . . . .	32
F.6. Survey Response Examples . . . . .	33
F.7. Conclusion . . . . .	36
G. Ablation Study on TIPO	37
G.1. Experimental Setup . . . . .	37
G.2. Evaluation Metrics . . . . .	37
G.3. Results & Discussion. . . . .	38
G.4. Speed Test and Overhead Analysis. . . . .	38
G.5. Conclusion of Ablation . . . . .	38
H. Topic Distribution Visualization	39
I . Discussion and Future Work	41

## A. Dataset/Resource

### A.1. Danbooru2023

The Danbooru2023 dataset [46, 68, 69] is an extensive collection of images and their corresponding tags, compiled from the Danbooru image board. This dataset includes images annotated with particular and detailed tags, providing a rich resource for training both the Text-to-Image (T2I) and Large Language Models (LLMs) involved in the TIPO framework. The dataset contains data up to image ID 7,349,999, encompassing various visual content with granular annotations. These annotations allow for creating nuanced and precise prompts, ensuring that longer, more detailed prompts can indicate subsets of shorter prompts.

#### Key Characteristics:

- **Rich Annotations:** Detailed tags differentiate subtle variations, crucial for specific image generation.
- **Large Volume:** Extensive dataset size ensures diverse training examples.
- **Tag-Based Prompting:** Refined prompts from detailed tags enhance image generation accuracy.

### A.2. GBC10M

The GBC10M dataset [29] is a large-scale collection of 10 million images sourced from CC12M [13], annotated using the Graph-Based Captioning (GBC) approach. Each image is represented by a graph where nodes correspond to object regions, compositions, and relations, and edges define their hierarchical relationships. Annotations are generated automatically through a pipeline leveraging pretrained multimodal large language models (MLLM) and object detection tools. The GBC structure enhances traditional image captions by providing detailed descriptions and structural information. Data is provided in JSON lines format, including image URLs, bounding boxes, and captions.

In TIPO, only the root node captions from GBC10M are utilized for concise yet descriptive prompts.

### A.3. Coyo HD 11M

The Coyo HD 11M dataset [12] consists of 11.4 million high-resolution, high-concept-density images paired with 22.8 million synthetic captions generated from the Coyo-700M dataset. Images maintain a minimum of 512 pixels on the shortest edge to ensure high visual quality. Captions, generated with the LLaVA-Next-8B model [38] based on LLaMA 3 [3], undergo post-processing for conciseness and clarity.

TIPO uses short and long captions, booru tags, and open image tags from this dataset.

### A.4. Stable Diffusion XL

Stable Diffusion XL (SDXL) [50] improves upon earlier models [56] with a more considerable UNet backbone and dual text encoders (CLIP ViT-L [51] and OpenCLIP ViT-bigG [31]), enhancing text conditioning. Supporting resolutions up to 1024×1024, SDXL accepts natural language prompts and tags, suitable for diverse image generation.

In this paper, three SDXL models are used without the refiner model:<sup>2</sup> SDXL-base-1.0<sup>3</sup>, Illustrious v3.5 - vpred<sup>4</sup>, and Kohaku-Zeta<sup>5</sup>.

### A.5. Illustrious

Illustrious is a series of fine-tuned Stable Diffusion XL models primarily trained on the Danbooru2023 dataset. In this study, we specifically employ the v3.5 version variant with v-parameterization [58], which is notable for its extensive incorporation of natural language prompts. The inclusion of both tag-based and natural language formats allows Illustrious to leverage a broad range of semantic knowledge for image generation.

Within TIPO, we perform an ablation study to analyze the effectiveness of different prompting strategies—namely extended tags versus natural language prompts—to identify which approach contributes most significantly to enhanced image generation performance.

---

<sup>2</sup><https://huggingface.co/stabilityai/stable-diffusion-xl-refiner-1.0>

<sup>3</sup><https://huggingface.co/stabilityai/stable-diffusion-xl-base-1.0>

<sup>4</sup>[OnomaAIResearch/Illustrious-xl-early-release-v0](https://github.com/OnomaAIResearch/Illustrious-xl-early-release-v0)

<sup>5</sup><https://huggingface.co/KBlueLeaf/Kohaku-XL-Zeta>

## A.6. Stable Diffusion 3.5

Stable Diffusion 3.5 (SD-3.5) incorporates the MMDiT architecture [20] and the Rectified Flow formulation [4, 36, 39] for improved text-to-image generation. Utilizing triple text encoders (CLIP/ViT-L, OpenCLIP/ViT-G, T5-XXL [52]), SD-3.5 supports resolutions up to  $1024 \times 1024$  and uses a 50/50 mix of original and CogVLM-generated captions. Figures confirm the capability to process both natural language prompts and tags.

This study employs SD-3.5-Large<sup>6</sup> (8B parameters) with FP8 inference on RTX 3090 or RTX 4090 GPUs.

## B. Implementation Details

In this appendix, we provide all the necessary details including our dataset construction process, model configurations, inference pipeline and the model’s properties not mentioned in Section 4.2 and 4.3.

### B.1. Training Data Construction

This section details our methodology for constructing and preprocessing training data to ensure robust model performance across various input scenarios.

**Length Control** To systematically control output prompt length, we implement a structured length categorization system using unique length tags. These tags enforce specific constraints on tag counts and natural language sentence lengths. For instance, the `<long>` tag specifies that the corresponding prompt must contain between 36 and 52 tags (inclusive), accompanied by 4 to 8 sentences of natural language description. We define four distinct length categories, each with strict bounds for tag count and sentence length.

Type	Very Short	Short	Long	Very Long
Tags (count)	18	36	48	72
NL (sentences)	2	4	8	18

Table 5. Maximum length specifications for each category and caption type. For each category, the actual count/length must not exceed these values.

**Random Augmentation** To enhance input diversity and better simulate real-world usage patterns, we implement several data augmentation strategies:

- **Metadata Tags:** For tags representing image metadata (e.g., artist, character, aspect ratio), we employ two randomization techniques:
  - Random removal of metadata tags
  - Random repositioning of metadata tags to the end of the prompt, after all content-related descriptionsThis approach encourages the model to handle varying metadata positions and availability, while maintaining the ability to infer metadata relationships from content descriptions.
- **Content Tags:** For tags describing image content (e.g., objects, actions, attributes), we implement:
  - Random shuffling of tag order within the content section
  - Length-based truncation to meet target length constraints while preserving key content information
- **Natural Language:** For natural language descriptions exceeding length limitations, we employ selective sentence removal, targeting middle sentences to preserve context-setting opening sentences and concluding details. This maintains coherent narrative flow while meeting target length requirements.

These augmentation strategies create a more diverse training dataset that better reflects real-world prompt variations, improving the model’s robustness and adaptability to different input styles and formats.

### B.2. Training Settings and Model Configurations

**Tokenizer and Task Tokens** TIPO employs a vocabulary derived from LLaMA2 [65] consisting of 32,000 tokens, with additional tokens (13 tokens) specifically designated for task and length control or placeholders. This extended vocabulary includes task identifiers and length modifiers to ensure flexibility across different prompt types:

<sup>6</sup><https://huggingface.co/stabilityai/stable-diffusion-3.5-large>

	TIPO-100M	TIPO-200M stage1	TIPO-200M stage2	TIPO-500M
Architecture	LLaMA			
Type	Pretrain	Pretrain	Finetune	Pretrain
Vocab Size	32013			
Hidden Dim	640	768	-	1280
Attention Heads	10	12	-	20
MLP Dim	2240	2304	-	3840
Hidden Layers	10	20	-	20
Model Parameters	100M	203M	-	508M
Max Learning Rate	5e-4	2e-4	5e-5	2e-4
Optimizer	AdamW			
LR scheduler	Cosine Annealing LR			
betas	0.9, 0.98			
weight decay	0.01			
Dataset	Coyo, GBC, Dan	GBC, Dan	Coyo, GBC, Dan	Coyo, GBC, Dan
Epoch	1	5	3	5
max context length	512	512	1024	1024
global batch size	1024	2048	2048	3584
Token Seen	6.0240B	22.625B	18.339B	31.274B
Hardware	4 × RTX3090	4 × RTX3090	4 × RTX3090	8 × H100
Training Time (wall)	22.5 hour	150 hour	270 hour	100 hour

Table 6. Training settings for TIPO models. The datasets include CoyoHD11M (Coyo), GBC10M (GBC), and Danbooru2023 (Dan). Stage 2 additionally incorporates Pixtral [1] to generate NL captions from Danbooru2023 dataset.

- **Placeholder Token (1 token):**

<|empty|>

- **Task Tokens (8 tokens):**

<|gen\_meta|>, <|tag\_to\_long|>, <|short\_to\_tag|>, <|long\_to\_tag|>, <|short\_to\_long|>, <|short\_to\_tag\_to\_long|>, <|short\_to\_long\_to\_tag|>, <|tag\_to\_short\_to\_long|>

- **Length Tokens (4 tokens):**

<|very\_short|>, <|short|>, <|long|>, <|very\_long|>

**Optimizer and Learning Schedule** Training is performed using the AdamW optimizer [40], with a cosine annealing learning rate scheduler [41]. The optimizer parameters include  $\beta_1 = 0.9$ ,  $\beta_2 = 0.98$ , and a weight decay of 0.01. Maximum learning rates are adjusted per model size, as outlined in Table 6.

**Training Configurations** TIPO models are trained in multiple stages. Table 6 summarizes the configurations for pretraining and fine-tuning TIPO-100M, TIPO-200M, and TIPO-500M. Both pretraining and fine-tuning was conducted on datasets like Danbooru2023 [46], GBC10M [29], and CoyoHD11M [12].

**Augmented Task Representation** Each dataset entry undergoes random task assignment and splitting to simulate a wide range of input-output mappings, effectively increasing the dataset size. For example, a single entry may contribute to tasks like `short_to_tag` or `tag_to_long`, with length modifiers dynamically controlling the output verbosity. This approach ensures the model can handle diverse tasks while maintaining robust generalization.

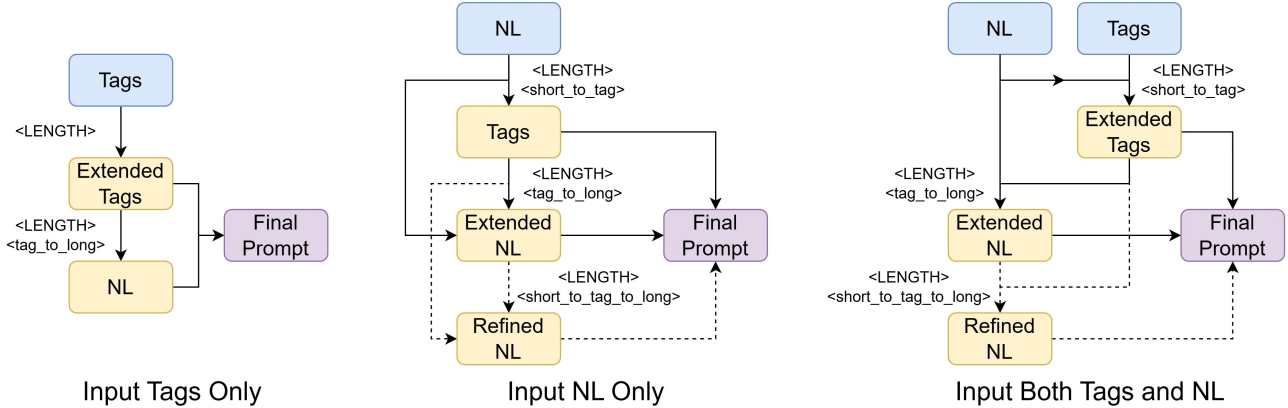


Figure 9. TIPO inference workflow, with solid arrows denoting the primary generation steps and dashed arrows indicating alternative generation paths within the same cycle. <TOKEN> represents special tokens, with all tokens detailed in Section B.2.

Hardware Platform	TIPO-100M		TIPO-200M		TIPO-500M	
	tok/sec	gen time	tok/sec	gen time	tok/sec	gen time
M1 Max (32 GPU cores)	339.4	0.66	190.0	1.23	119.4	2.02
RTX 3090	558.5	0.42	341.4	0.69	289.8	0.81
RTX 4090	742.9	0.29	454.5	0.51	359.7	0.63

Table 7. Model performance comparison across different hardware platforms. Tokens per second (tok/sec) represents the average generation speed, while generation time (gen time) shows the average time in seconds required for a complete two-step prompt optimization process.

**Hardware and Time Requirements** Training was conducted on NVIDIA RTX3090 GPUs for smaller models and H100 GPUs for TIPO-500M. Total wall-clock training times ranged from 22.5 hours for TIPO-100M to 270 hours for fine-tuning TIPO-200M.

**Token Seen and Effective Training** Non-padding tokens are used to measure the effective token count during training, ensuring efficiency given the short and variable data lengths. Table 6 details the total tokens seen per model and training stage, illustrating the comprehensive exposure to diverse data entries.

### B.3. Inference Pipeline

The TIPO inference pipeline is designed to handle various input types and scenarios, combining different tasks to refine or expand both tag-based and natural language prompts. Figure 9 illustrates this comprehensive workflow.

Our framework processes tags and natural language inputs separately, allowing for specialized handling of each input type. This flexible pipeline allows TIPO to adapt to various input scenarios, whether the user provides tags, natural language descriptions, or both. By leveraging different task combinations, TIPO ensures that tag-based and natural language prompts are optimized, resulting in more detailed and effective input for text-to-image models.

### B.4. Model Speed Comparison

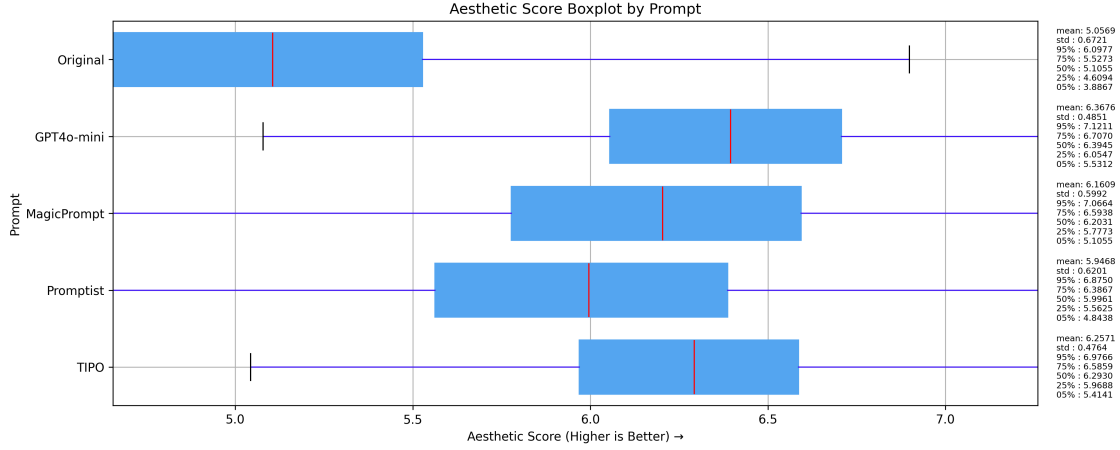
We conducted comprehensive speed tests of our 100M, 200M and 500M parameter models using the inference pipeline described in Section 5.2. Each prompt requires two sequential generation steps. Our primary metric is average tokens generated per second, which reflects real-world task performance rather than theoretical maximum throughput.

The evaluation was performed using llama.cpp [23], an efficient C++ implementation that provides optimized support for various hardware accelerators including CUDA, HIP, and Apple Metal.

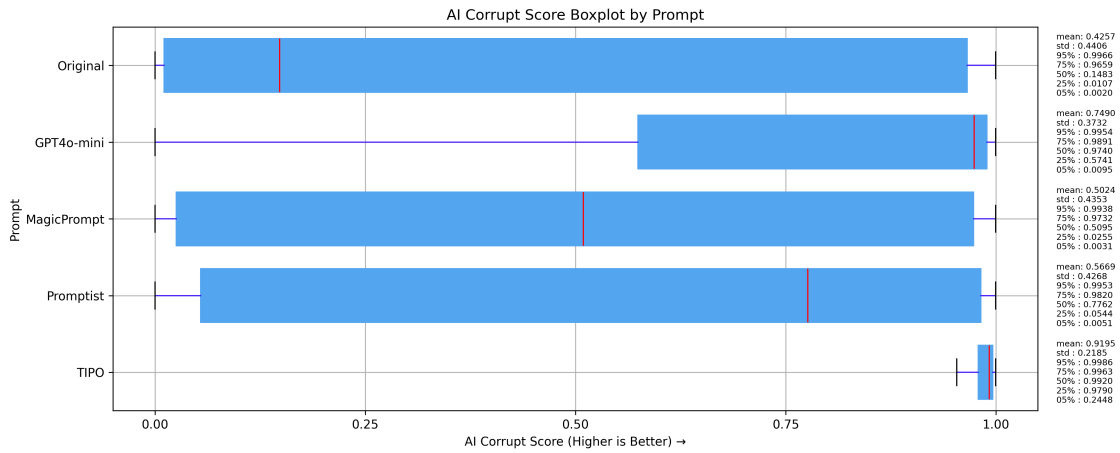
## C. Evaluation Statistics

In this appendix, we provide more statistics for the result obtained in Section 5.

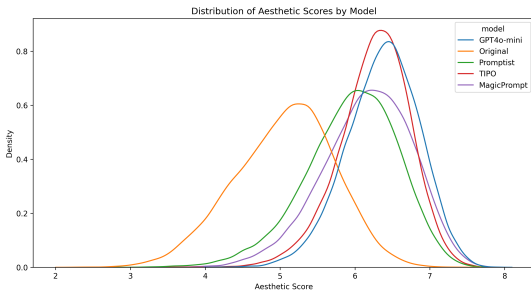
### C.1. In-domain test regarding scenery tag



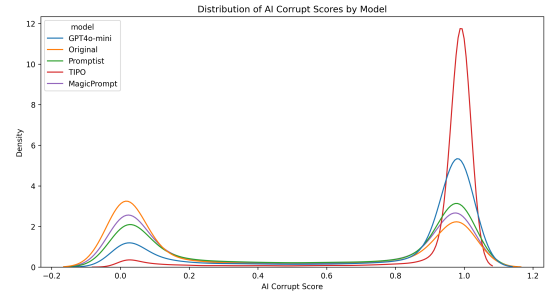
(a) The box plot for the Aesthetic Score result of scenery tag test.



(b) The box plot for the AI Corrupt Score result of scenery tag test.



(c) The KDE plot for the Aesthetic Score result of scenery tag test.

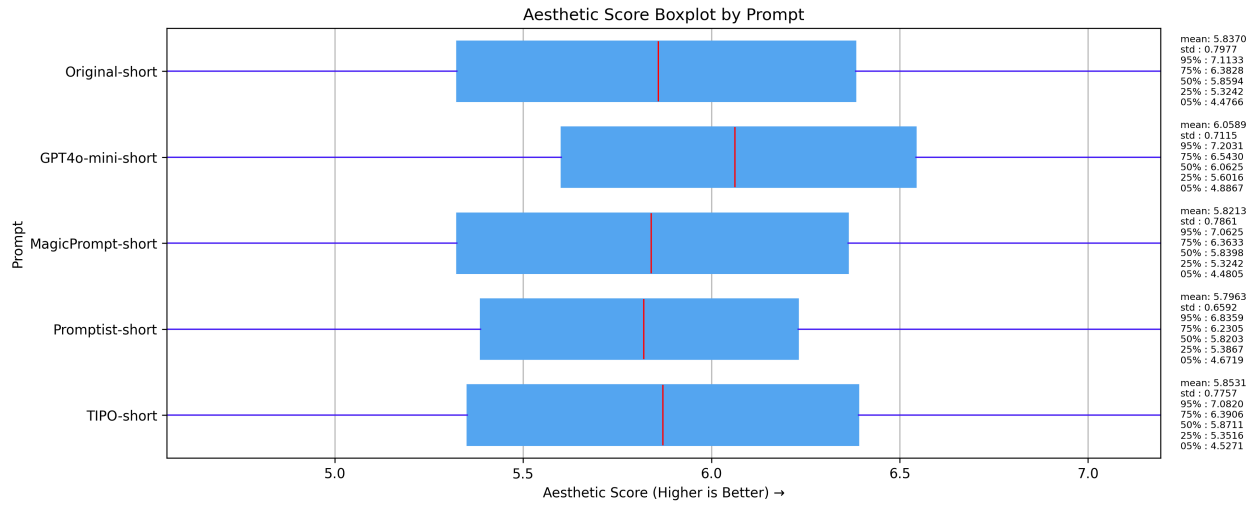


(d) The KDE plot for the AI Corrupt Score result of scenery tag test.

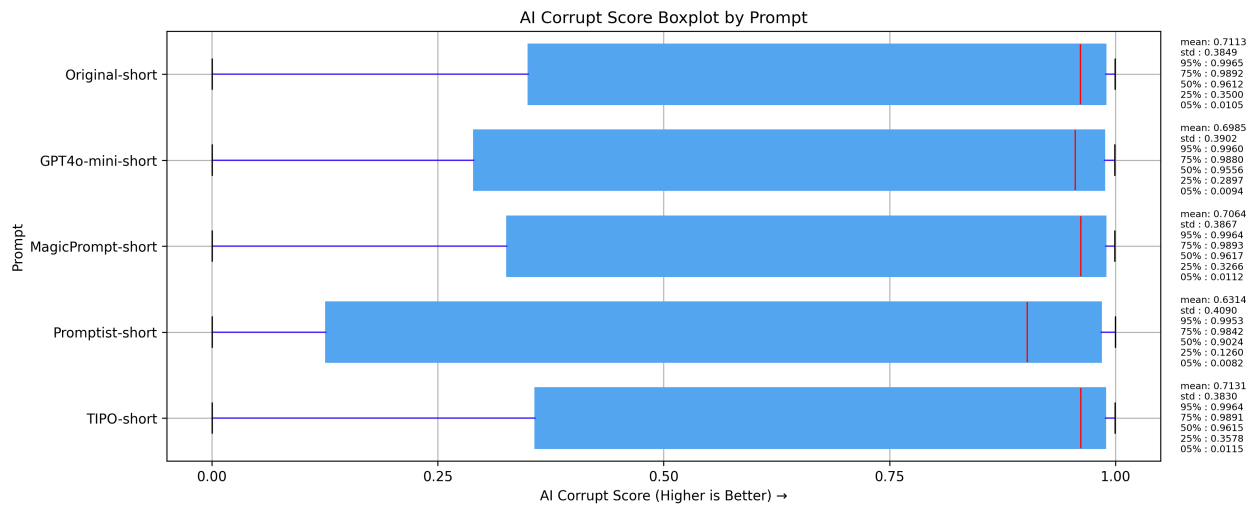
Figure 10. The distribution of aesthetic and AI corrupt score for scenery tag test.

The box plot and Kernel Density Estimation (KDE) plot displayed in Figure 10 illustrate the aesthetic scores and AI corruption scores from the scenery tag test described in Section 5.2. The analysis shows that TIPO significantly outperforms all other methods, demonstrating a considerable margin of improvement.

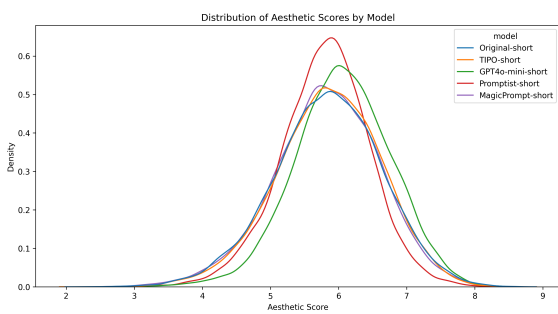
## C.2. In-domain prompt generation test



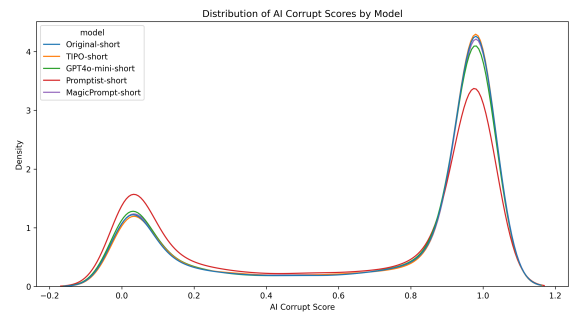
(a) The box plot for the Aesthetic Score result of short prompt input.



(b) The box plot for the AI Corrupt score result of short prompt input.

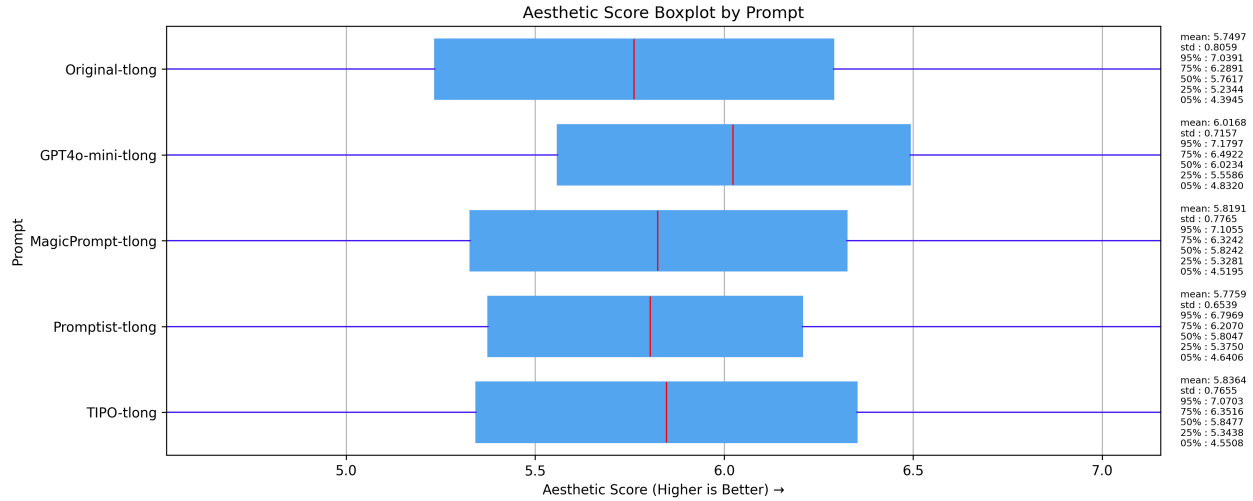


(c) The KDE plot for the Aesthetic Score result of short prompt input.

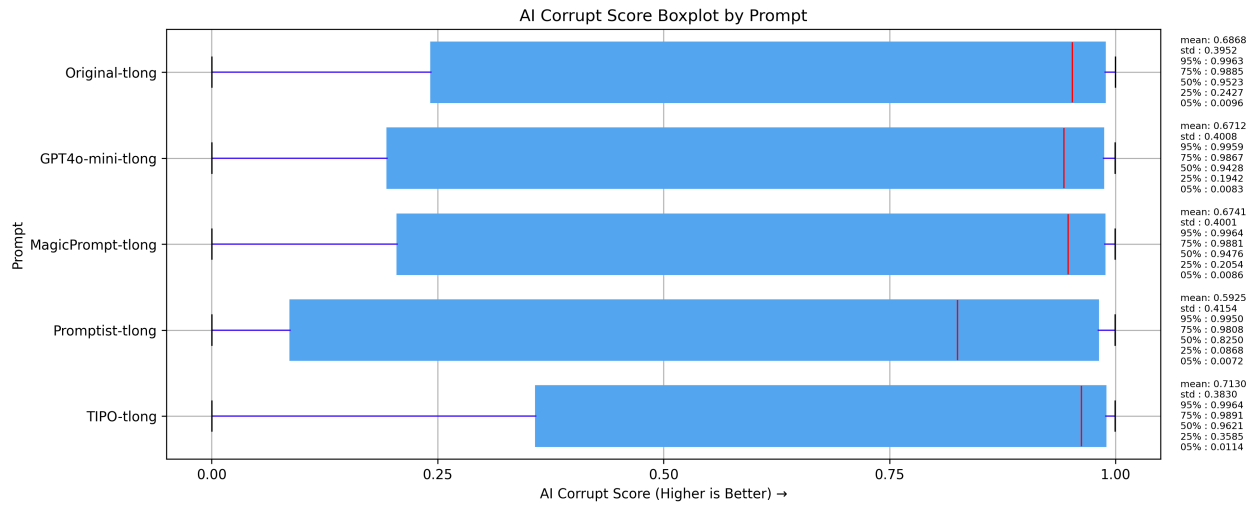


(d) The KDE plot for the AI Corrupt Score result of short prompt input.

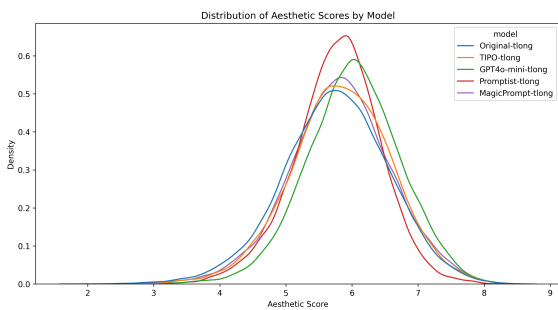
Figure 11. The distribution of aesthetic and AI corrupt score for short prompt input.



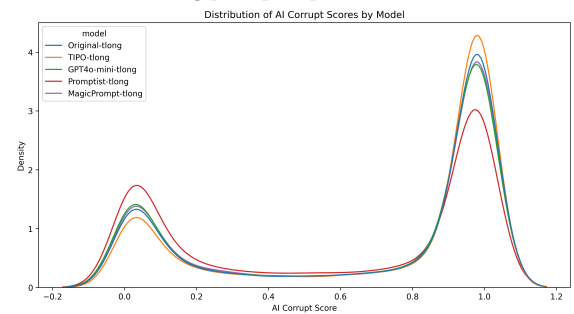
(a) The box plot for the Aesthetic Score result of truncated long prompt input.



(b) The box plot for the AI Corrupt score result of truncated long prompt input.



(c) The KDE plot for the Aesthetic Score result of truncated long prompt input.

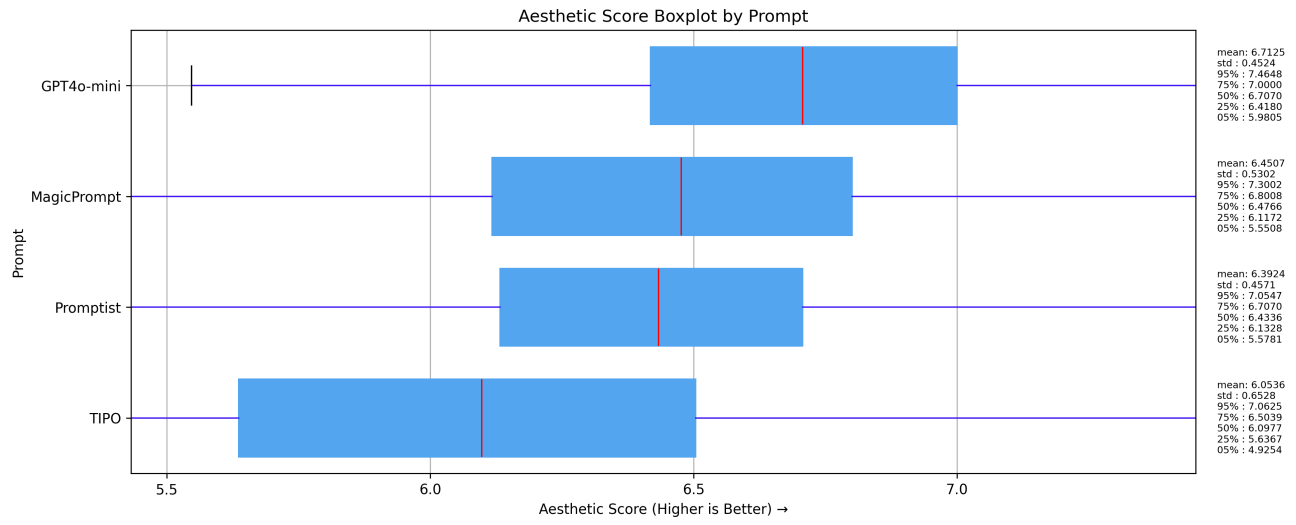


(d) The KDE plot for the AI Corrupt Score result of truncated long prompt input.

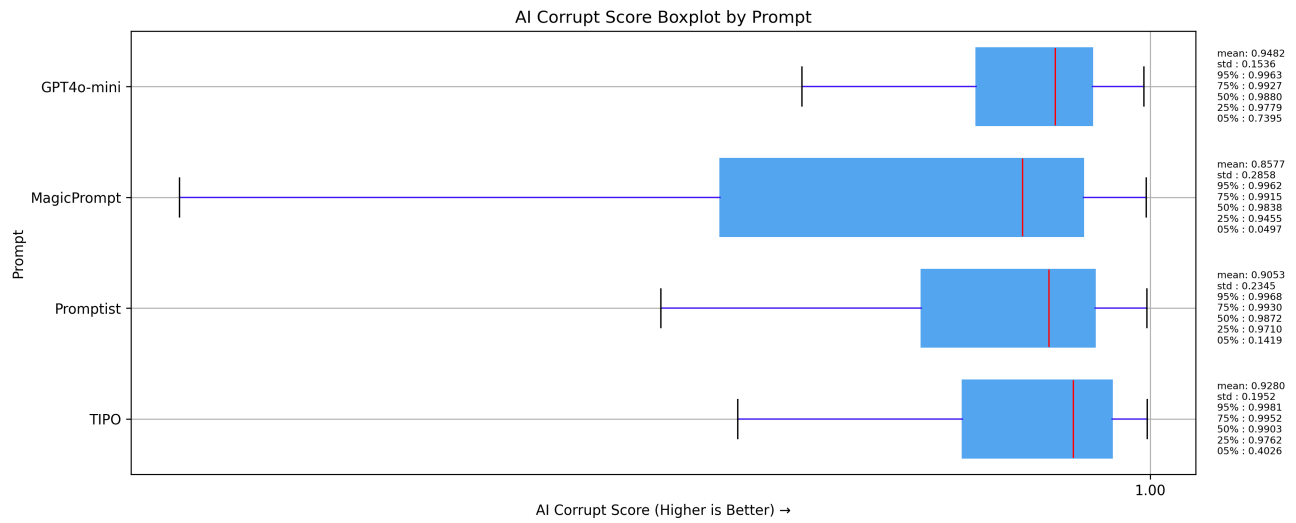
Figure 12. The distribution of aesthetic and AI corrupt score for truncated long prompt input.

Figures 11 and 12 display the box plots and KDE plots of aesthetic scores and AI corruption scores obtained from the In-domain prompt generation test detailed in Section E.2. While the box plots reveal subtle differences in performance between various methods, the AI corruption scores provide valuable insights. Specifically, these scores indicate that implementations supported by TIPO produce more stable output images than other methods.

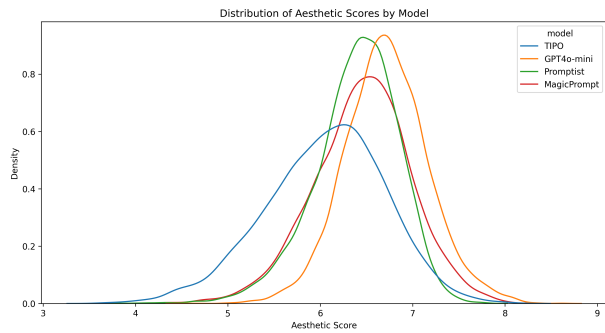
### C.3. Out-of-domain evaluation



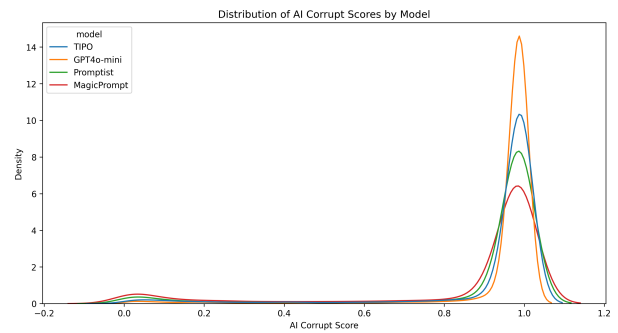
(a) The box plot for the Aesthetic Score result of out-of-focus test.



(b) The box plot for the AI Corrupt Score result of out-of-focus test.



(c) The KDE plot for the Aesthetic Score result of out-of-focus test.



(d) The KDE plot for the AI Corrupt Score result of out-of-focus test.

Figure 13. The distribution of aesthetic and AI corrupt score for out-of-focus test.

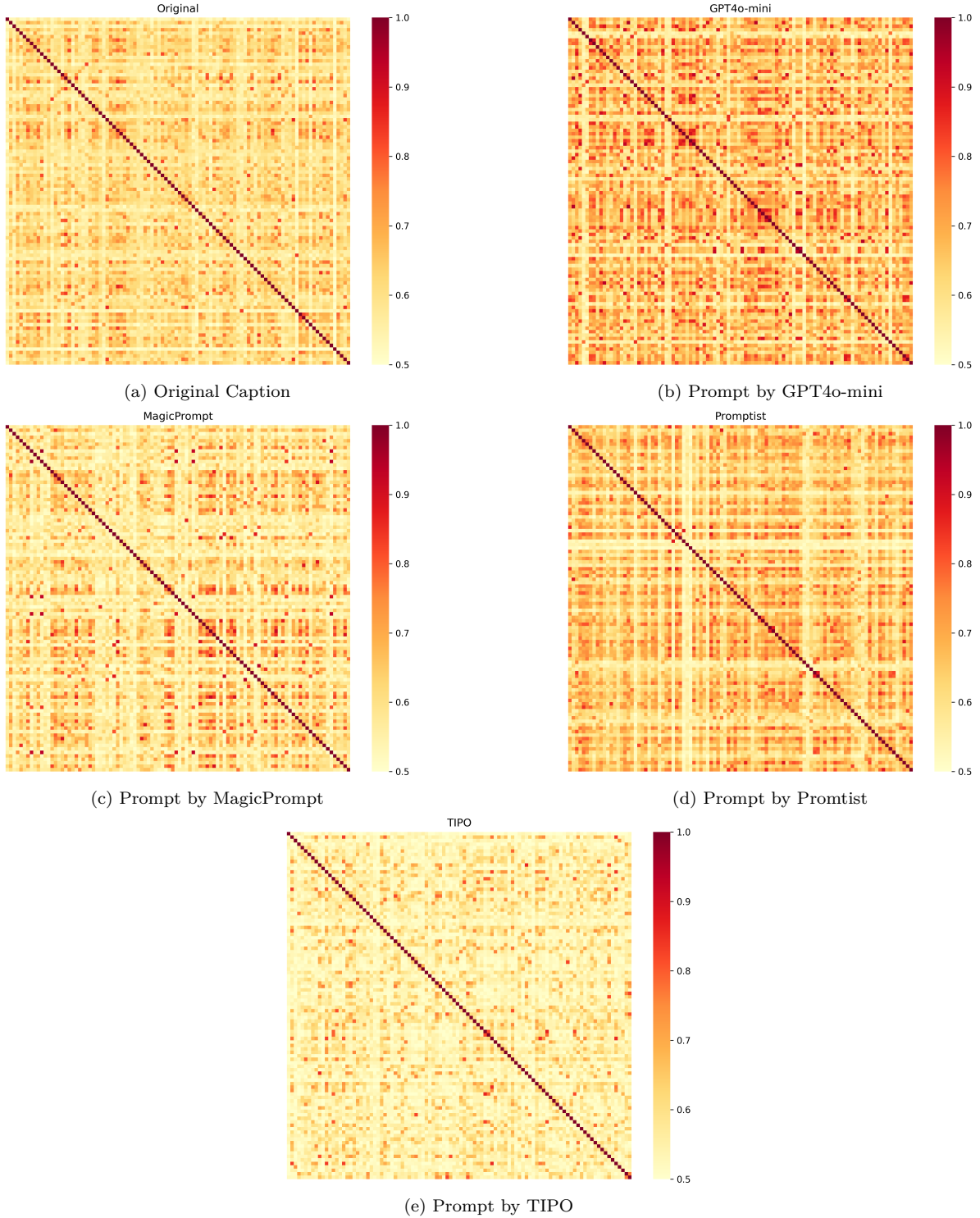


Figure 14. The similarity matrix for the 100 best aesthetic results generated in the SD3.5-Large experiments. Off-diagonal elements of the matrix indicate the similarity between different images. A lower value for an off-diagonal element indicates greater diversity among the generated images.

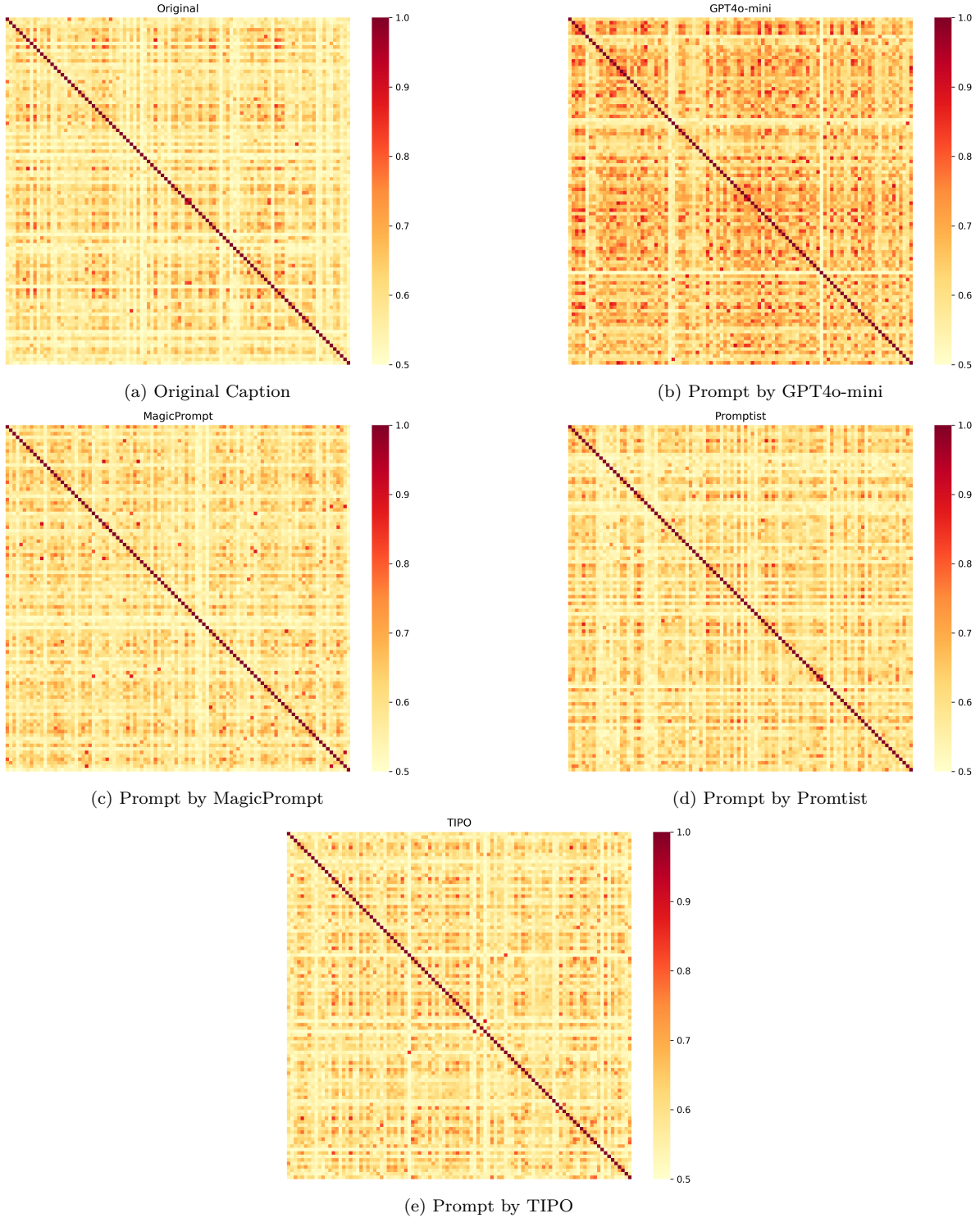
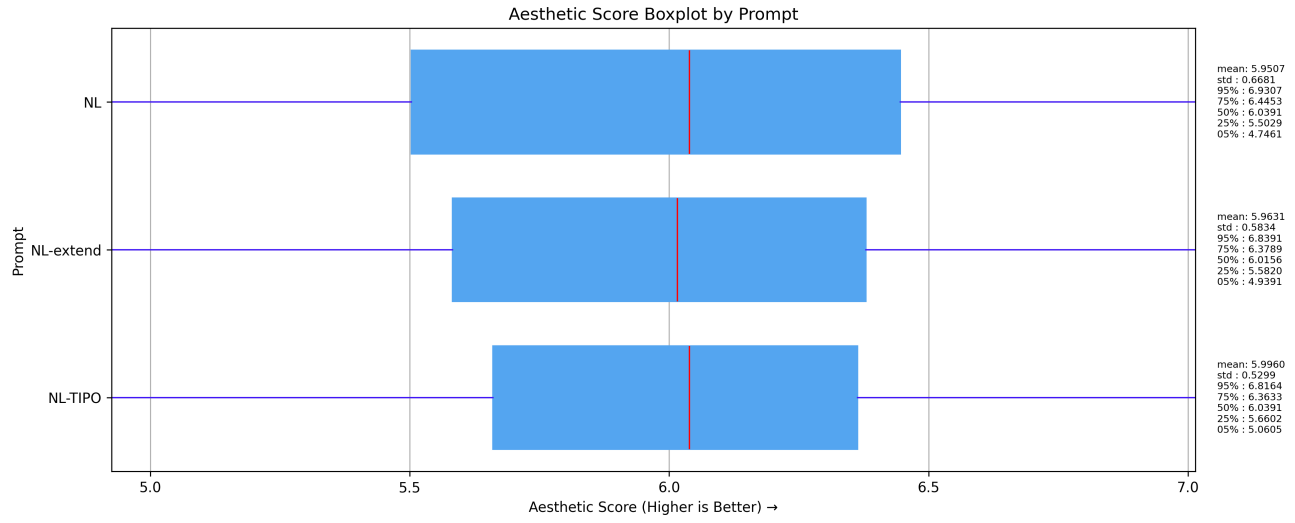


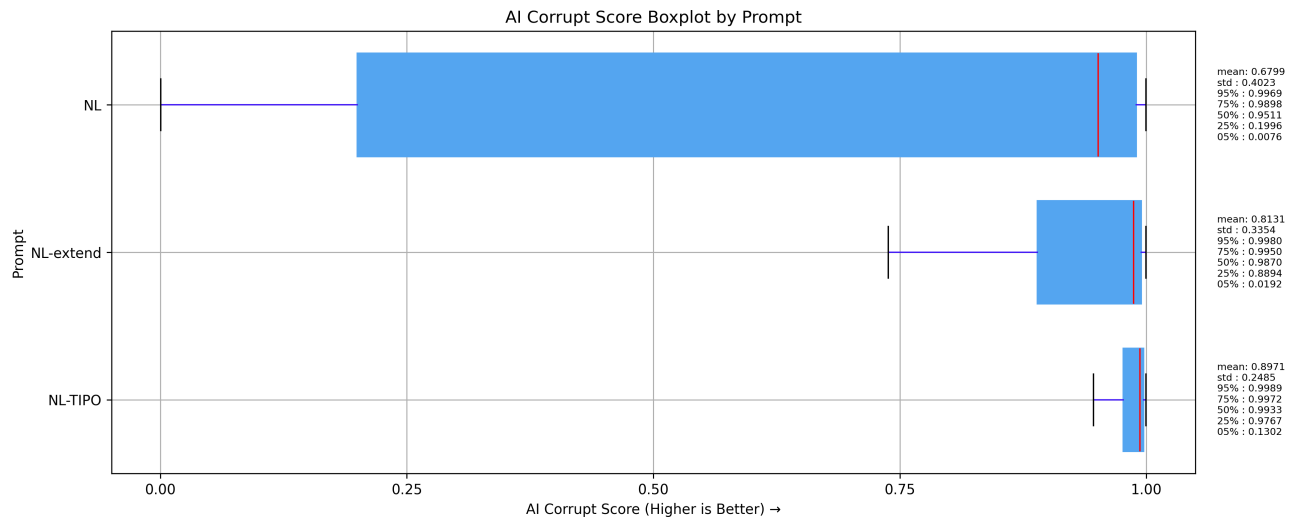
Figure 15. The similarity matrix between 100 images of worst aesthetic generated results of SD3.5-Large experiments.

Figures 14 and 15 present similarity matrices for different prompt generation methods and their corresponding aesthetic outputs on SD3.5-Large [21]. A matrix with predominantly lower similarity values (brighter appearance) indicates high diversity among generated images, while higher values (darker appearance) suggest consistent but less diverse outputs. Please refer to Table 3 in Section 5.

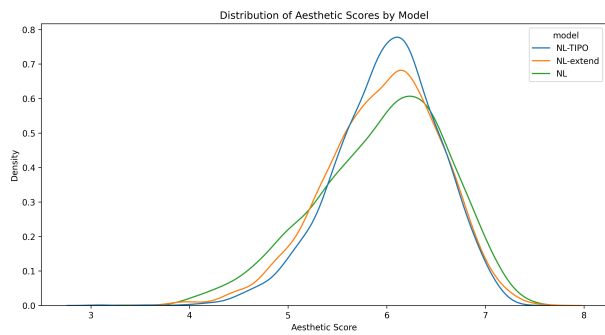
## C.4. Ablation Test



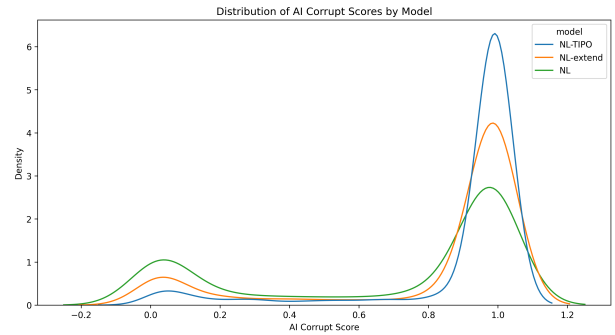
(a) The box plot for the Aesthetic Score result of NL ablation test.



(b) The box plot for the AI Corrupt Score result of NL ablation test.

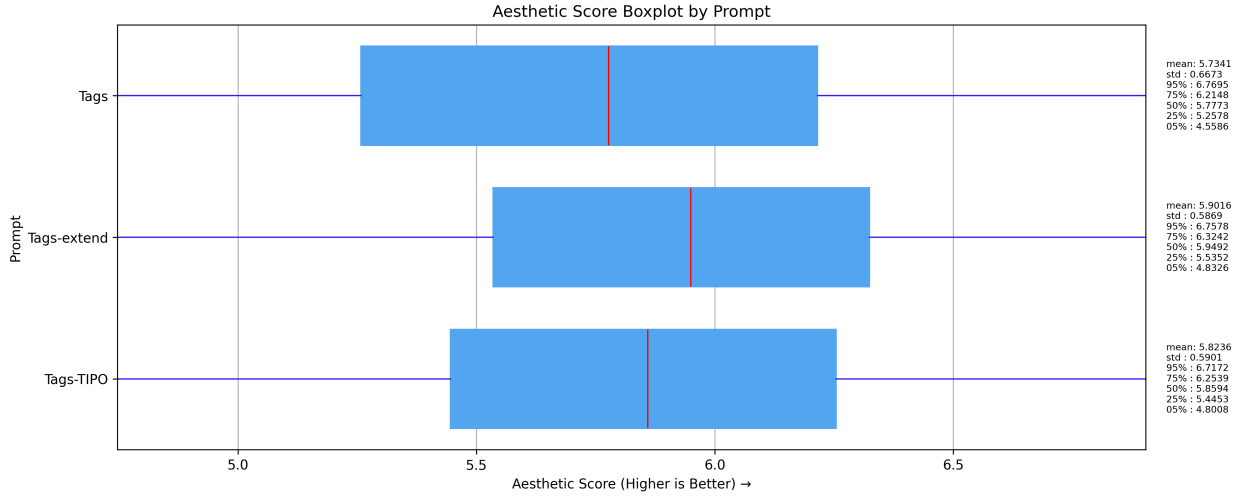


(c) The KDE plot for the Aesthetic Score result of NL ablation test.

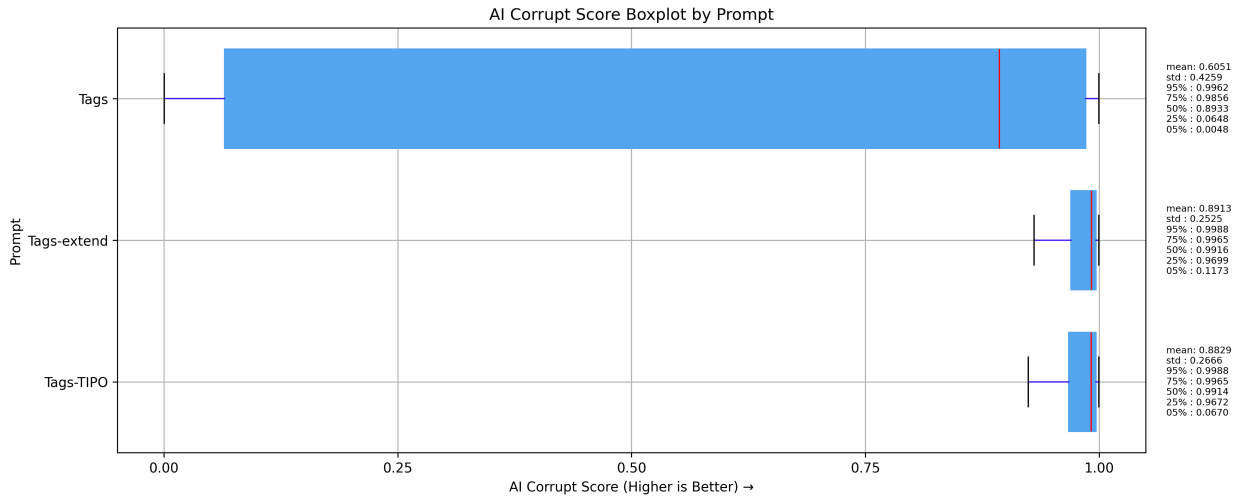


(d) The KDE plot for the AI Corrupt Score result of NL ablation test.

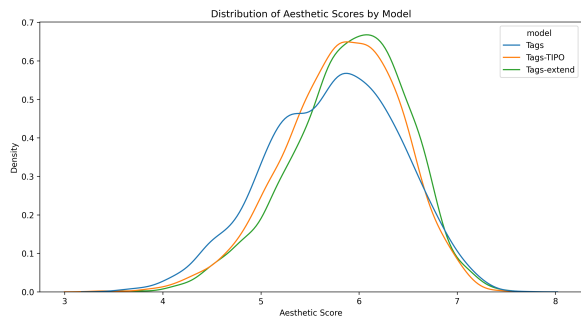
Figure 16. The distribution of aesthetic and AI corrupt score for NL ablation test.



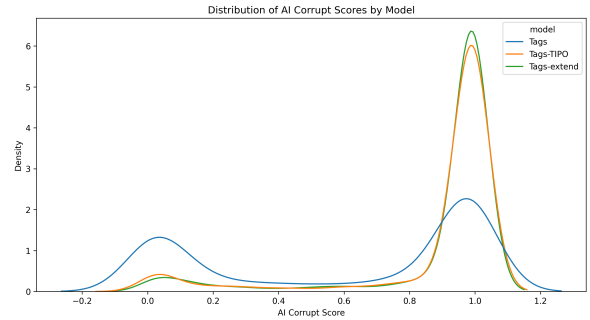
(a) The box plot for the Aesthetic Score result of tags ablation test.



(b) The box plot for the AI Corrupt Score result of tags ablation test.



(c) The KDE plot for the Aesthetic Score result of tags ablation test.



(d) The KDE plot for the AI Corrupt Score result of tags ablation test.

Figure 17. The distribution of aesthetic and AI corrupt score for tags ablation test.

Figures 17 present the tag ablation test in the TIPO effect on the aesthetic score and AI Corrupt Score among the original tag, tag-extend and the tags TIPO. The box plot reveals that the tag TIPO is better than the original tag and the tag extend is the best. In detail, KDE plot reveals that the tag TIPO has a similar performance compared with the tag extend. Both of them are better than the original tag, which indicates that the tag TIPO aspect helps control corruption and promotes the aesthetic score.

## D. TIPO example

In this section, we provide some text example of TIPO's input and output.

**TIPO Format Template**

**User Input:**  
1girl, ciloranko, maccha (mochancc), ningen mame, ask (askzy), solo, masterpiece, absurdres, newest, safe

A girl sits in a cozy cafe, cradling a cup of coffee in her hand

---

**Formatted TIPO Input for Expand Tags:**  
meta: absurdres  
rating: safe  
artist: ciloranko, maccha (mochancc), ningen mame, ask (askzy)  
quality: masterpiece, newest  
aspect\_ratio: 1.0  
target: <|short|> <|short\_to\_tag|>  
short: A girl sits in a cozy cafe, cradling a cup of coffee in her hand  
tag: 1girl, solo

---

**Formatted TIPO Output after Expand Tags and Expand Natural Prompt:**  
meta: absurdres  
rating: safe  
artist: ciloranko, maccha (mochancc), ningen mame, ask (askzy)  
quality: masterpiece, newest  
aspect\_ratio: 1.0  
target: <|short|> <|tag\_to\_long|>  
tag: 1girl, solo, sitting, closed mouth, jewelry, long hair, looking at viewer, crossed legs, plant, table, couch, bracelet, cup, smile, teacup, indoors, blue eyes, blonde hair, holding  
long: A girl sits in a cozy cafe, cradling a cup of coffee in her hand. The cafe has large windows with green plants on the walls and a wooden table in front of her. Behind her is a staircase leading to another room. The overall atmosphere of the image is serene and inviting.

---

**Formatted Output for Text-to-Image:**  
1girl, ciloranko, maccha (mochancc), ningen mame, ask (askzy),  
solo, sitting, closed mouth, jewelry, long hair, looking at viewer, crossed legs, plant, table, couch, bracelet, cup, smile, teacup, indoors, blue eyes, blonde hair, holding,  
A girl sits in a cozy cafe, cradling a cup of coffee in her hand. Behind her is a staircase leading to another room. The cafe has large windows with green plants on the walls and a wooden table in front of her. The overall atmosphere of the image is serene and inviting.



User Input



TIPO Output

masterpiece, newest, absurdres, safe

Figure 18. An example of formatted content used for training and inference in TIPO.

## TIPO Format template

### User Input:

scenery , no humans , masterpiece , absurdres , newest , safe

### Formatted TIPO Input For Expand Tags:

```
meta: absurdres
rating: safe
quality: masterpiece, newest
aspect_ratio: 1.0
target: <|long|>
tag: scenery, no humans
```

### Formatted TIPO Output after Expand Tags and tag\_to\_long task:

```
meta: absurdres
rating: safe
quality: masterpiece, newest
aspect_ratio: 1.0
target: <|long|> <|tag_to_long|>
tag: scenery, no humans, storefront, motor vehicle, road sign, power lines, plant, railing, flower pot,
vanishing point, outdoors, sign, potted plant, sidewalk, awning, tree, bicycle, window, railroad
crossing, bush, building, utility pole, lamppost, shop, truck, traffic light, fence, chinese text,
stairs, door, bicycle basket, town, day, streetcar (cafe), lamp, road
long: A small town with a variety of buildings and houses. the sky is blue and there are trees in the
background. on the left side of the image, there is an orange building with a sign that reads "
chinese restaurant". on the right side, there are several other buildings with different types of
shops and restaurants. in front of the buildings, there appears to be a street with cars parked
along the road.
```

in the center of the illustration, we can see a train crossing signal with two red lights and a blue sky above it. there is also a yellow building with white walls and a green roof. on top of the traffic light pole, there seems to be an air conditioning unit. the street is lined with trees and bushes, and there is graffiti on the ground.

### Formatted Output For Text-to-Image

```
scenery, no humans, storefront, motor vehicle, road sign, power lines, plant,
railing, flower pot, vanishing point, outdoors, sign, potted plant,
sidewalk, awning, tree, bicycle, window, railroad crossing, bush,
building, utility pole, lamppost, shop, truck, traffic light, fence,
chinese text, stairs, door, bicycle basket, town, day, streetcar \ (cafe) \
, lamp, road,
```

A small town with a variety of buildings and houses. the sky is blue and there are trees in the background. on the left side of the image, there is an orange building with a sign that reads "chinese restaurant". on the right side, there are several other buildings with different types of shops and restaurants. in front of the buildings, there appears to be a street with cars parked along the road. in the center of the illustration, we can see a train crossing signal with two red lights and a blue sky above it. there is also a yellow building with white walls and a green roof.

masterpiece, newest, absurdres, safe



User Input



TIPO Output

Figure 19. An example formatted content we used for training and inference in TIPO.

## E. Image Examples

In this section, we present sample images from the experiments described in Section 5 to visually demonstrate the improvements achieved by TIPO.

### E.1. In-domain test regard to scenery tag

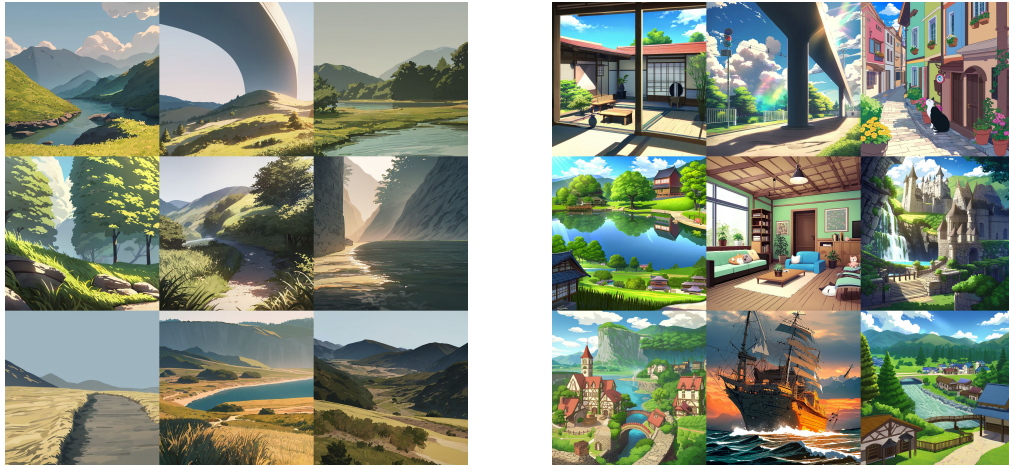


Figure 20. Comparison of generated images using simple input (left) vs. TIPO-enhanced input (right) for the scenery tag

Figure 20 demonstrates the difference in output diversity between simple input and TIPO-enhanced input for the scenery tag. As observed, TIPO significantly expands the range of generated sceneries, better reflecting the variety present in the Danbooru2023 dataset [69]. The left column shows results from simple input (scenery tag only), while the right column illustrates the enhanced diversity achieved with TIPO-enhanced input.

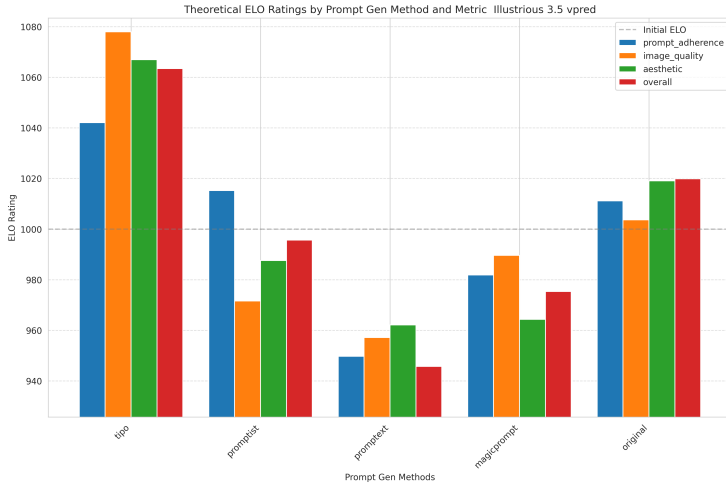
### E.2. In-domain prompt generation test



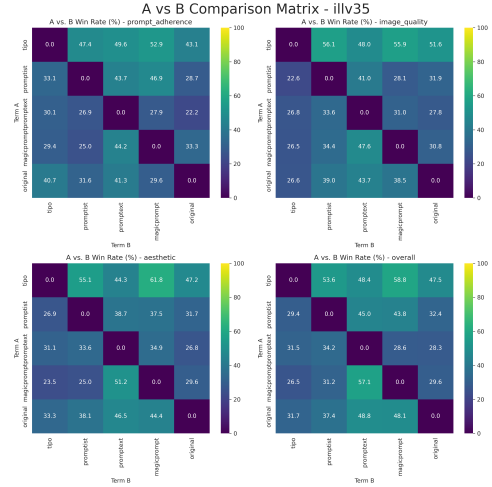
Figure 21. Comparison of generated images using original input (left) vs. TIPO-enhanced input (right)

Figure 21 illustrates the differences between short captions, truncated long captions, TIPO-generated captions, and TIPO-extended captions. The “short prompt” and “truncated long prompt” used in this experiment typically consist of 1-2 sentences, resulting in reasonably good quality outputs. However, the use of TIPO to refine or extend these prompts still yields noticeable improvements in aesthetics and overall quality.

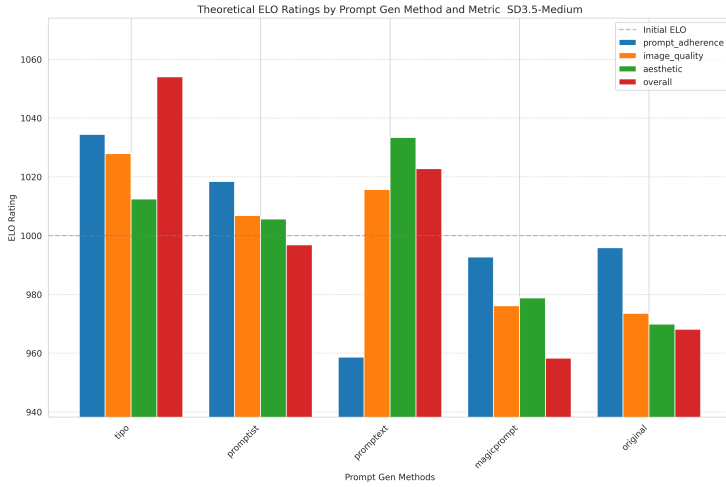
## F. Human Preference



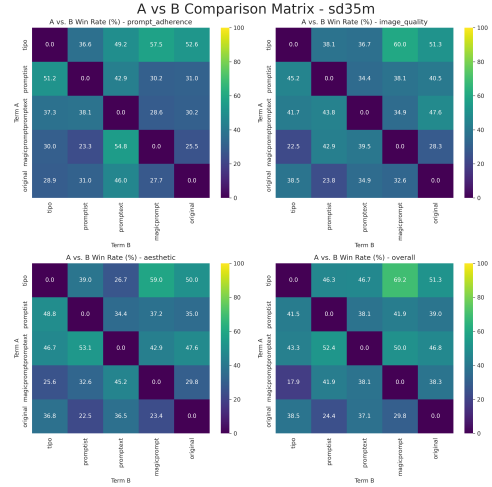
(a) ELO rating on Illustrious



(b) Win rate matrix on Illustrious



(c) ELO rating on SD3.5-medium



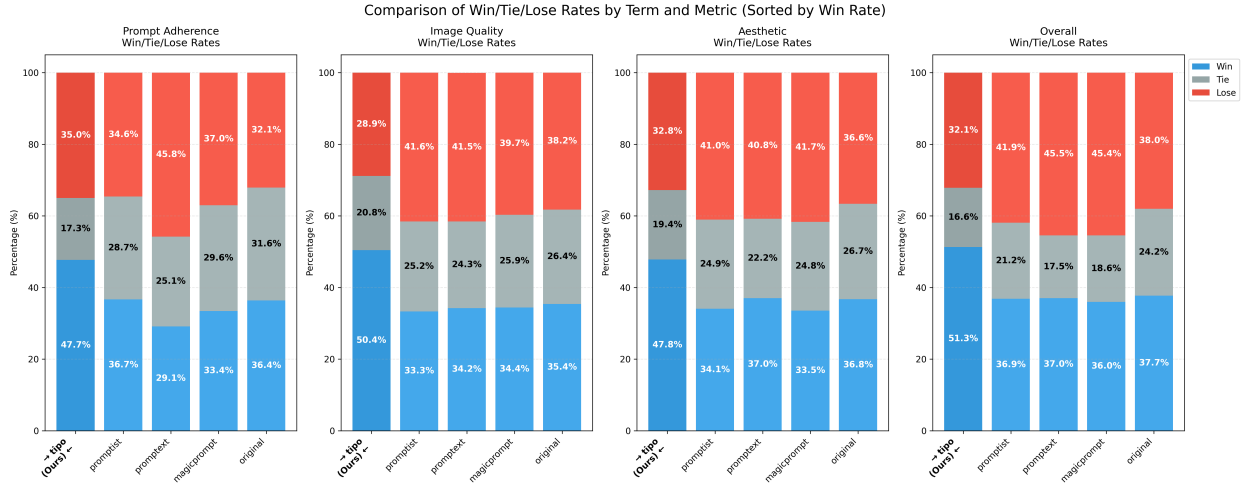
(d) Win rate matrix on SD3.5-medium

Figure 22. ELO ratings and win rate matrices across different experimental settings comparing five prompting methods (TIPO, Promptist, Prompttext, MagicPrompt, and Original) on three evaluation dimensions

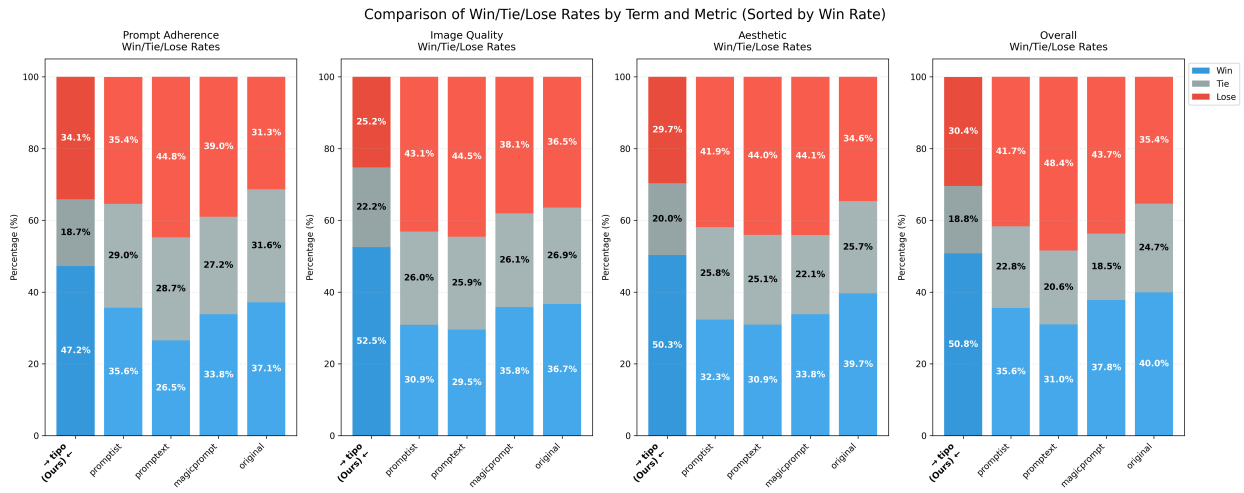
We conducted a series of A/B tests to compare five prompt transformations, (*TIPO*, *Promptist*, *Prompttext*, *MagicPrompt*, and *Original(unmodified)*), for two models, *Illustrious*, *SD3.5-medium*, which is known for both core word/natural language understanding. In total, we collected responses for  $\sim 1,500$  pairwise comparisons, from more than 20 anonymous evaluators. Each evaluation asked participants to compare two generated images—labeled *A* and *B*—and select which they preferred (or a tie) according to specific criteria (e.g., prompt adherence, image quality, or aesthetic appeal).

### F.1. User Interface for Human Preference Evaluation

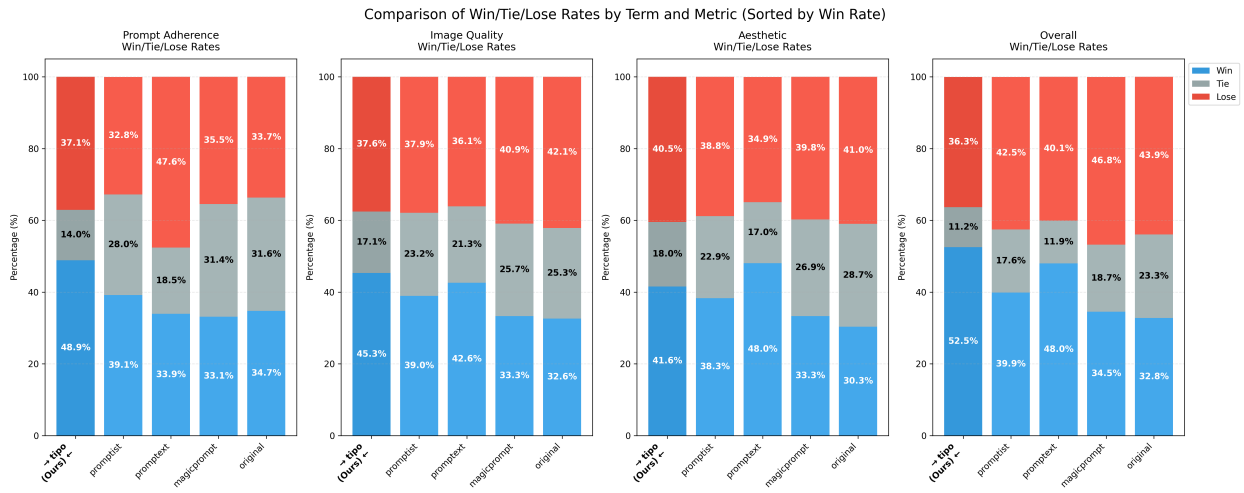
We developed a specialized survey interface to facilitate efficient and unbiased human evaluation of generated images. As illustrated in Figure 24, the interface presents evaluators with an original prompt and two corresponding images (labeled *A* and *B*) generated using different prompting methods. Before submission, users can see the original prompt in the center panel while the processed prompts used to generate each image remain hidden to prevent bias.



(a) Full Win-Tie-Lose plot

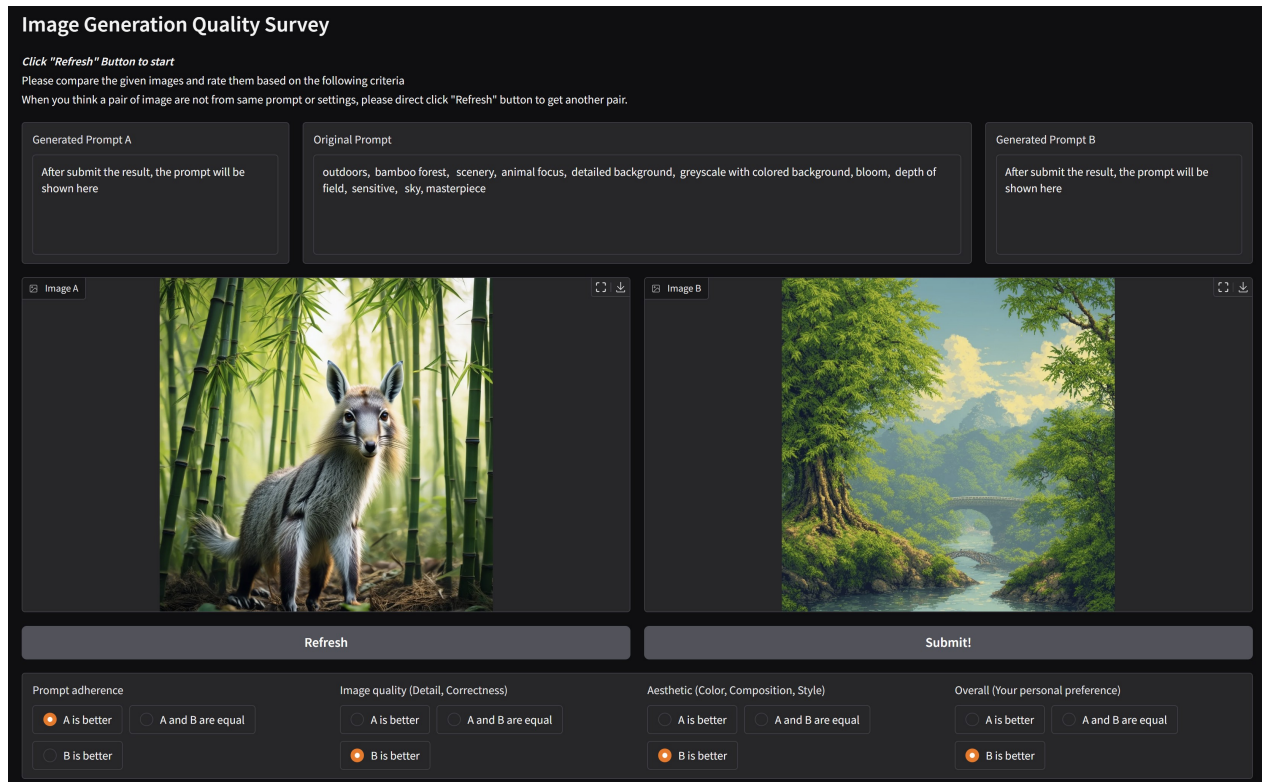


(b) Illustrious Win-Tie-Lose plot

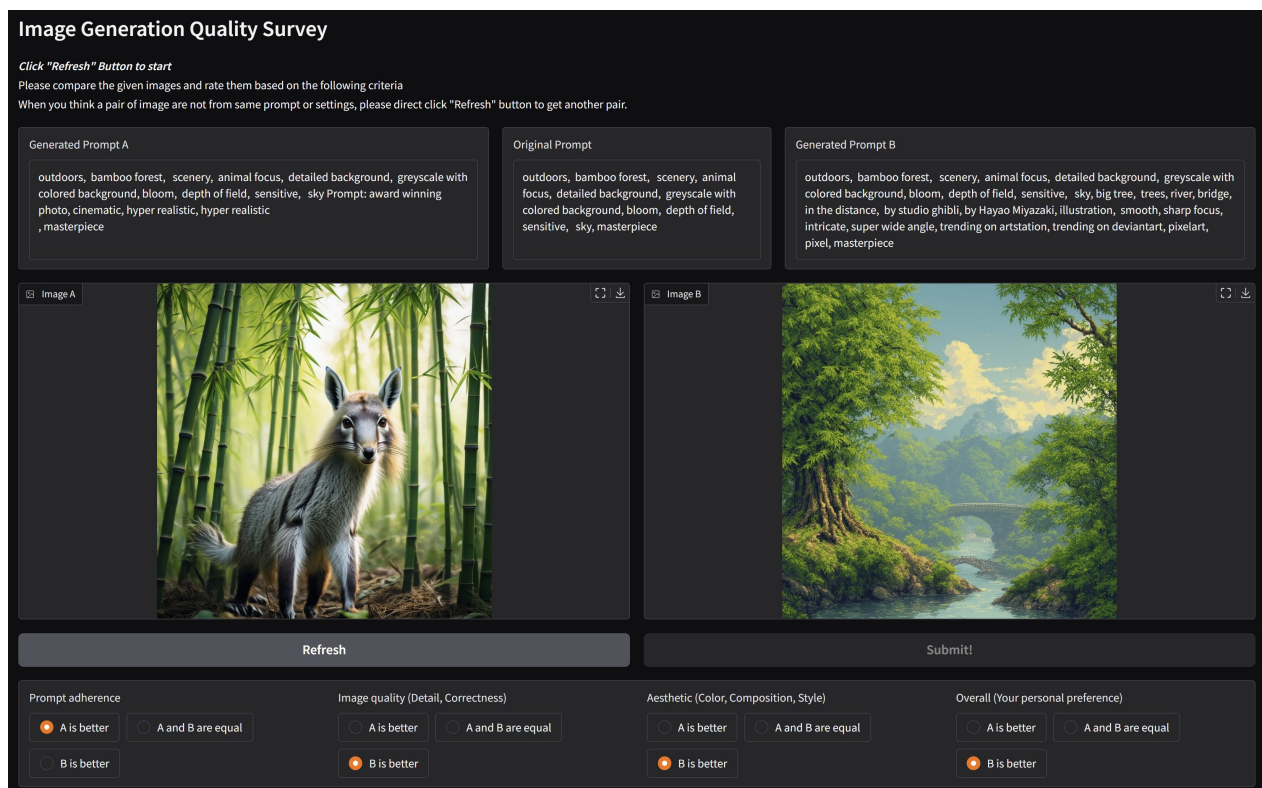


(c) SD3.5-medium Win-Tie-Lose

Figure 23. Win-Tie-Lose comparison across different experimental settings showing the relative performance of five prompting methods on prompt adherence, image quality, and aesthetic appeal metrics



(a) The UI of survey system before submitting the choices.



(b) The UI of survey system after submitting the choices.

Figure 24. Survey interface for human evaluation of image pairs, showing the evaluation process before submission (a) where users compare two images based on four metrics, and after submission (b) where the generated prompts for each image are revealed

Comparison	Win Ratio (A:B)	Proportion A	$p$ -value	Significant?
Original vs. PromptExtend	45:66	0.405	0.0572	Marginally
Original vs. Tipo	28:80	0.259	< 0.0001	Yes***
Original vs. Promptist	35:64	0.354	0.0046	Yes**
PromptExtend vs. Promptist	41:80	0.339	0.0005	Yes***
Promptist vs. Tipo	30:101	0.229	< 0.0001	Yes***
PromptExtend vs. Tipo	30:90	0.250	< 0.0001	Yes***
MagicPrompt vs. Promptist	14:34	0.292	0.0055	Yes**
MagicPrompt vs. Tipo	11:48	0.186	< 0.0001	Yes***
MagicPrompt vs. Original	15:28	0.349	0.0660	No
MagicPrompt vs. PromptExtend	19:35	0.352	0.0402	Yes*

Table 8. Pairwise win rates and statistical significance (Overall Dimension). *Significance levels: \*  $p < 0.05$ , \*\*  $p < 0.01$ , \*\*\*  $p < 0.001$*

The evaluation framework requires participants to compare the image pairs across four distinct metrics: prompt adherence (how well the image follows the original prompt), image quality (detail and correctness), aesthetic appeal (color, composition, and style), and overall personal preference. For each metric, users can select one of three options: “A is better,” “A and B are equal,” or “B is better.”

When evaluators encounter image pairs that appear to be from different prompts or settings, they are instructed to click “Refresh” to obtain a new comparison. After submitting their evaluations, the interface reveals the transformed prompts used to generate each image, providing transparency about how the original prompt was modified by each method.

## F.2. Extended Human Evaluation.

Participants assessed each image’s performance on prompt adherence, image quality, and aesthetic appeal, with visually shown unmodified and image pairs. TIPO exhibited superior outcomes in all comparison settings. Notably, it attained a 64.4% peak win rate (against MagicPrompt) under the Full scenario and 57.5% (also against MagicPrompt) under SD35-medium, emphasizing TIPO’s proficiency in generating images that closely follow prompt specifications while maintaining visual coherence.

## F.3. ELO Ratings.

We computed theoretical ELO ratings from the aggregated pairwise comparisons to quantify overall performance differences among the five methods. The rating update rules were based on each pair’s binary outcome (win or lose), ignoring tie cases. The result is depicted in Figure 22, TIPO has secured the highest ELO rating over other models.

## F.4. Human Preference ELO Method

We computed theoretical ELO ratings from human-judged pairwise preference data to quantitatively evaluate the relative performance of each prompting method. The ELO rating system, initially designed for ranking chess players, aggregates binary outcomes into numerical ratings representing comparative performance.

**Pairwise Outcomes.** Human evaluators assessed comparisons between methods, resulting in one of three outcomes:

- Method  $i$  wins: assigned a score of 1 for method  $i$ , and 0 for method  $j$ .
- Method  $j$  wins: assigned score 1 for method  $j$ , and 0 for method  $i$ .
- Tie: assigned score 0.5 to both methods.

**Conversion to ELO Differences.** Win and tie rates were converted to ELO rating differences using:

$$\text{Adjusted Win Rate} = \text{Win Rate} + \frac{\text{Tie Rate}}{2}$$

$$\text{ELO Difference} = 400 \times \log_{10} \left( \frac{\text{Adjusted Win Rate}}{1 - \text{Adjusted Win Rate}} \right)$$

To ensure numerical stability, extreme adjusted win rates were constrained as follows:

$$\text{ELO Difference} = \begin{cases} -800, & \text{Adjusted Win Rate} \leq 0.001 \\ +800, & \text{Adjusted Win Rate} \geq 0.999 \end{cases}$$

**Calculating Method ELO Ratings.** Final ELO ratings were determined by averaging each method’s pairwise ELO differences and centering these averages around a baseline rating (e.g., 1000):

$$\text{ELO}_{\text{method}_i} = \text{Base Rating} + (\text{Average ELO Difference for method } i - \text{Overall Mean ELO Difference})$$

**Interpretation of ELO Scores.** Methods with higher ELO scores consistently outperform lower-scored methods. A rating difference of 400 points corresponds to a 90% expected win probability for the superior method.

## F.5. Statistical Significance

As summarized in Table 8, we conducted two-sided binomial and McNemar’s tests ( $p < 0.05$ ) to assess the statistical significance of observed differences. The result confirms that TIPO’s advantages are unlikely to be explained by random variation, which also supports a consistent performance hierarchy: TIPO ranks highest, followed by Promptist, PromptExtend, Original, and MagicPrompt. Collectively, these findings illustrate TIPO’s robust, model-agnostic effectiveness and underscore the model-sensitivity of alternative methods, particularly Promptext and MagicPrompt.

## F.6. Survey Response Examples

In this section we provided some responses of our human preference survey as reference.

best quality, absurdes, indoors, flower shop, animal focus, detailed background, colorful background, general  
colorful background, general, dark, sky, night, anaglyph, masterpiece  
masterpiece

Image A



Image B



Prompt Adherence:  
B is better

Image Quality:  
B is better

Aesthetic:  
A is better

Overall:  
B is better

outdoors, animal focus, detailed background, gradient backgroundshade, shadow, darkness, bloom, depth of field  
bloom, depth of field, sensitive, dark, cafe, anaglyph, scenery, depth of field  
scenery, depth of field, masterpiece

Image A



Image B



Prompt Adherence:  
A is better

Image Quality:  
A is better

Aesthetic:  
A is better

Overall:  
A is better

Figure 25. Some survey responses on illustrious-3.5-vpred generated image with different prompt optimization method

semirealistic, 1girl, high-waist skirt, headphones, detailed background, rainbow background, bloom, depth of field  
bloom, depth of field, sensitive, fishes, transparent, scenery, backlighting, masterpiece  
backlighting, masterpiece

Image A



Image B



Prompt Adherence:  
A and B are equal

Image Quality:  
A and B are equal

Aesthetic:  
B is better

Overall:  
B is better

house, entrance, 1girl, Top Hat, bow, detailed background, rainbow background, sensitive  
rainbow background, sensitive, classroom, fading, masterpiece

Image A



Image B



Prompt Adherence:  
A and B are equal

Image Quality:  
A and B are equal

Aesthetic:  
A and B are equal

Overall:  
B is better

Figure 26. Some survey responses on illustrious-3.5-vpred generated image with different prompt optimization method

semirealistic, scenery, animal focus, detailed background, two-tone backgroundshade, shadow, darkness, bloom  
darkness, bloom, depth of field, general, sketch, scratch art, coffee, fading  
coffee, fading, masterpiece

Image A



Image B



Prompt Adherence:  
A is better

Image Quality:  
B is better

Aesthetic:  
A is better

Overall:  
A is better

shrine, scenery, animal focus, detailed background, rainbow background, sensitive, sketch, scratch art  
sketch, scratch art, funeral, fading, scenery, muted colors, greyscale, masterpiece  
greyscale, masterpiece

Image A



Image B



Prompt Adherence:  
A is better

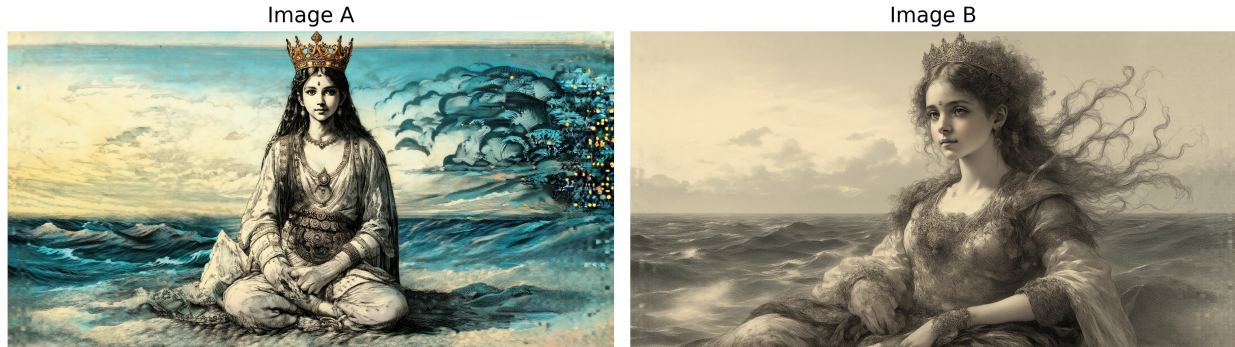
Image Quality:  
A is better

Aesthetic:  
A and B are equal

Overall:  
A is better

Figure 27. Some survey responses on SD3.5-medium generated image with different prompt optimization method

semirealistic, 1girl, Jodhpurs, crowns, detailed background, greyscale with colored background, general, sketch  
general, sketch, scratch art, ocean, fading, masterpiece



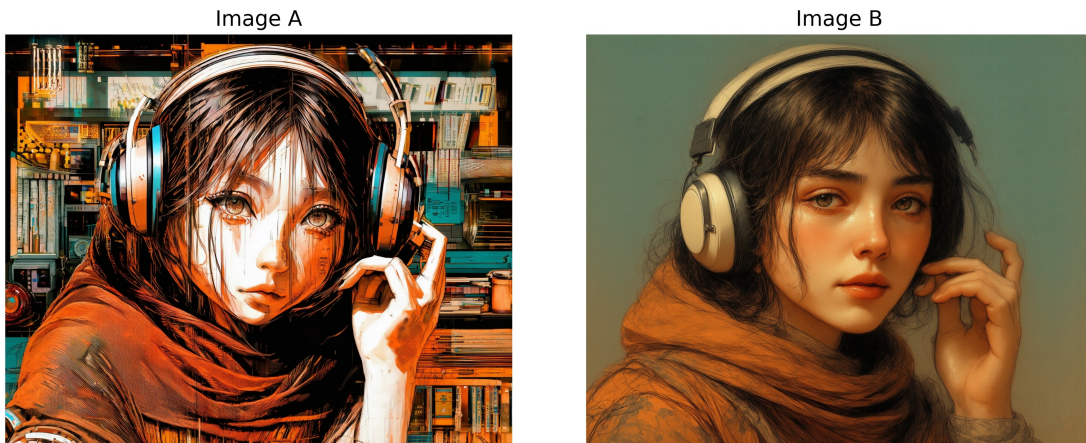
Prompt Adherence:  
B is better

Image Quality:  
B is better

Aesthetic:  
B is better

Overall:  
B is better

extremely aesthetic, 1girl, Jubbah, headphones, detailed background, multicolored backgroundshade, shadow, darkness  
shadow, darkness, general, sketch, scratch art, coffee, transparent, scenery  
transparent, scenery, JPEG artifacts on purpose, masterpiece



Prompt Adherence:  
A and B are equal

Image Quality:  
B is better

Aesthetic:  
A is better

Overall:  
A is better

Figure 28. Some survey responses on SD3.5-medium generated image with different prompt optimization method

## F.7. Conclusion

The extended evaluations presented here reinforce TIPO's standing as a reliable and effective prompt-optimization strategy. Its consistent performance gains under diverse model conditions highlight its potential for broad applicability, with its strong alignment with user-specified prompts, high image quality, and favorable aesthetic outcomes.

## G. Ablation Study on TIPO

In this section, we investigate the effect of incorporating **TIPO** (Tags + Inferred Prompt Objects) across various generation settings. Our primary goal is to validate whether additional structured information (e.g., core tags and minimal spatial/contextual cues) can improve image quality, reduce artifacts.

### G.1. Experimental Setup

**Prompt Variants.** To systematically analyze TIPO’s contribution, we consider four types of input prompts improvement task:

1. *Tag*  $\rightarrow$  *More core words*: Given an initial set of core words, generate more refined or expanded core words.
2. *NL*  $\rightarrow$  *More NL*: Given a short natural language (NL) description, elaborate into a richer NL prompt.
3. *Tag*  $\rightarrow$  (*More core words + NL*): Combine expanded tags with a corresponding NL description derived from them.
4. *NL*  $\rightarrow$  (*More NL + core words*): Use the NL prompt to add relevant tags, forming a mixed prompt of NL plus core words.

In each case, we compare the baseline prompts (without TIPO cues) against prompts incorporating TIPO’s structured, tag-based critical information and minimal spatial hints.

**Data Preparation.** We start by randomly sampling core words from a word table to represent a diverse range of topics (e.g., objects, environments, descriptors). Additionally, for each word set, we generate a corresponding short NL sentence using a compact language model (GPT4o-mini). Overall, the six prompt variants are tested on 4,000 images, ensuring a balanced comparison.

**Inference Procedure.** Prompts are fed into our image-generation pipeline under identical model settings (classifier free guidance, sampler, steps, etc.), using the v-parameterized variant of *Illustrious v3.5* [49]. We focus on how TIPO modifications alter the generation outcomes and whether they introduce additional computational overhead.

### G.2. Evaluation Metrics

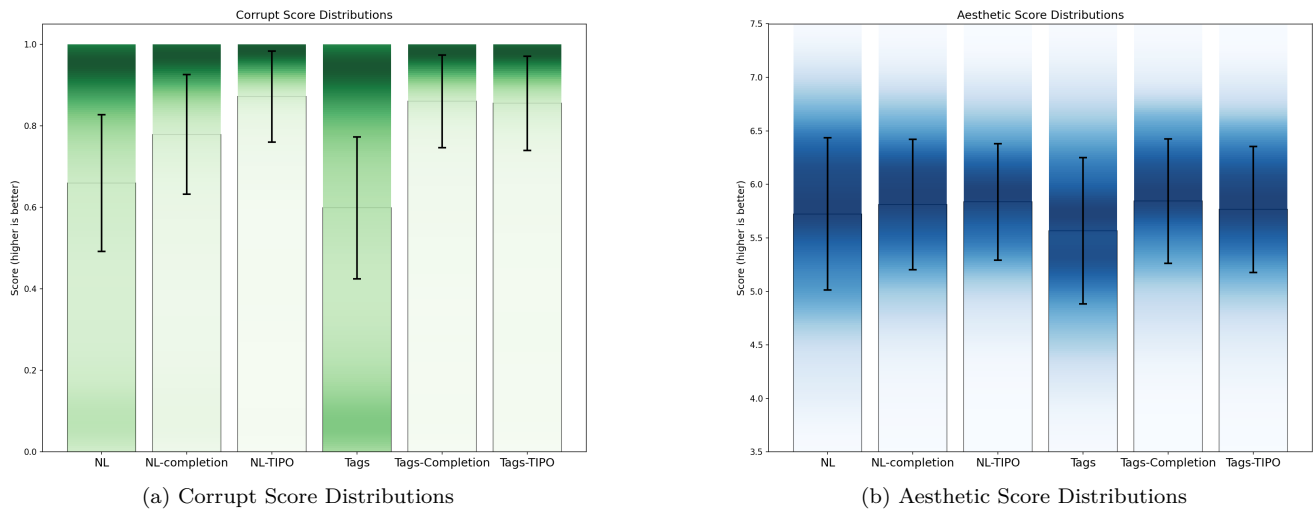


Figure 29. Side-by-side comparison of Corrupt (left) and Aesthetic (right) score distributions across prompt types.

**Aesthetic Score.** We employ an off-the-shelf aesthetic predictor to estimate image quality. In the following paragraph, we discuss the model’s bias.

**AI Corruption Score.** Using an automated ‘AI corruption’ detection model, we measure generation artifacts, such as distorted objects and unnatural shapes. Higher scores imply cleaner, more coherent outputs.

### G.3. Results & Discussion

**Impact on Aesthetics.** Figure 29b shows that **TIPO**-enhanced prompts generally achieve higher aesthetic scores than their non-TIPO counterparts, albeit with some variance. Notably, we observe a correlation between wider color ranges and higher aesthetic scores discussed in Figure 30, suggesting a bias toward more colorful or varied compositions.

**Improvements in Corruption Score.** As shown in Figure 29a, **TIPO**-based prompts yield significantly lower corruption scores, indicating fewer artifacts. We hypothesize that the additional spatial and contextual details encoded via **TIPO** help the model place objects more consistently.

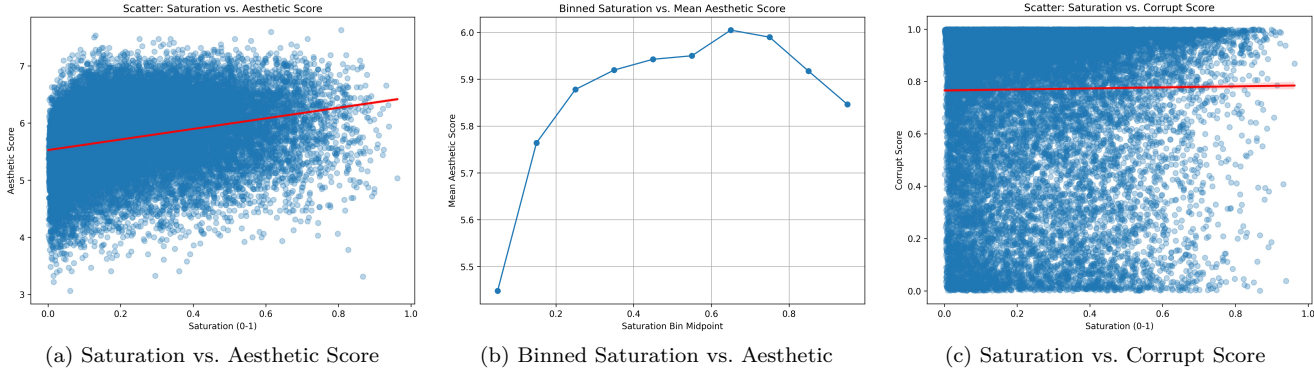


Figure 30. Scatter plots (left and right) and binned analysis (middle) showing the relationship between saturation and image metrics. We find a moderate positive correlation between saturation and aesthetic score (Pearson  $r = 0.2821$ ), particularly at lower saturation ranges, based on 24k samples. However, saturation shows no notable correlation with corrupt score (Pearson  $r = 0.0125$ ).

### G.4. Speed Test and Overhead Analysis

A key concern for production pipelines is whether **TIPO** generation imposes a substantial time overhead. We benchmarked prompt-generation inference on four smaller models, excluding any large proprietary LLMs. As illustrated in Table 9, the additional **TIPO**-related computation remains well below the image-generation time. Hence, even in a synchronous pipeline, **TIPO** prompt expansion does not constitute a bottleneck.

Table 9. Speed Test Results for **TIPO** and Other Prompt Methods

Method	Model/Config	# Runs	Avg. Time (s)	Std. Dev. (s)
TIPO	LLaMA-500M	500	1.4207	1.0730
	LLaMA-200M	200	1.0306	0.8982
	LLaMA-100M	200	1.0078	0.9394
PROMPTIST	GPT2-125M	1000	1.4593	0.2857
PROMPTTEXTEND	GPT2-125M	1000	1.3849	0.2151
MAGICPROMPT	GPT2-125M	1000	1.1398	0.4043

**Memory Footprint.** We also confirm that **TIPO**'s overhead in terms of VRAM usage is minimal. The practical adoption of **TIPO** in pipelines has shown no critical memory concerns, which aligns with our measurements.

### G.5. Conclusion of Ablation

Our experiments suggest that **TIPO** (1) consistently lowers AI corruption artifacts, (2) can boost aesthetic scores, and (3) remains computationally inexpensive. The improvements in metrics support the viability of **TIPO** prompts

for real-world image-generation tasks. In short, a concise natural language prompt with core tag-based critical information appears to be an effective, suggested form for most use cases.

## H. Topic Distribution Visualization

Latent Dirichlet Allocation (LDA) [9] is a generative probabilistic model for topic modeling [32], which assumes that each document is a mixture of topics, with each topic represented by a distribution over words. LDA uncovers hidden thematic structures by analyzing word co-occurrence patterns, while methods like TF-IDF and TextRank [43] enhance its ability to extract meaningful insights from large textual datasets. We implemented a multi-stage topic modeling and clustering methodology using LDA to extract varying numbers of topics (20, 30, 50, and 100) from the corpus. This approach focuses on identifying significant representative words while filtering out stop words and irrelevant terms to ensure meaningful topic classification.

We empirically assessed whether the resulting topics were sufficiently large and diverse by employing multi-level topic analysis. This iterative process mitigates potential challenges such as substantial topic overlap, which can diminish distinctiveness when extracting a large number of topics [62].

To address the potential overlap and further assess the diversity and meaningfulness of the topics, we performed a secondary clustering [70]. We grouped the initially extracted topics into five major clusters using k-means clustering. We evaluated the clustering performance by calculating the inertia (Sum of Squared Distances) [27], shown in Table 10, 11, and 12. Since the topics have already been filtered for meaningful content, a higher inertia value indicates greater diversity among the clusters, reflecting a broader range of valid and meaningful topics across the dataset. This two-tiered approach allows for a more nuanced analysis of topic diversity and ensures the robustness of the topic modeling against meaningless word groupings.

Size	MagicPrompt		GPT4o-mini		Promptist		TIPO	
	Run 1	Run 2	Run 1	Run 2	Run 1	Run 2	Run 1	Run 2
20	170.78	137.94	1078.38	204.71	125.90	144.59	1037.44	271.77
30	461.79	417.74	1758.40	736.74	327.48	195.13	1323.88	512.07
50	829.68	730.73	861.15	1036.33	400.90	373.74	823.51	959.18
100	1656.74	1245.60	1987.63	1628.32	877.36	657.14	1622.79	1777.61

Table 10. Inertia for COYO-Dataset inference, higher is better

Size	MagicPrompt		GPT4o-mini		Promptist		TIPO	
	Run 1	Run 2	Run 1	Run 2	Run 1	Run 2	Run 1	Run 2
20	184.53	352.16	244.79	246.15	125.47	198.94	278.56	211.98
30	452.01	566.74	505.56	441.34	204.28	328.70	372.07	471.28
50	571.77	895.47	1227.30	990.17	438.89	313.48	737.65	788.41
100	1291.60	1742.36	1675.41	1550.32	631.61	628.78	1573.47	1855.90

Table 11. Inertia for GBC-Dataset inference, higher is better

Size	MagicPrompt	GPT4o-mini	Promptist	TIPO
20	60.82	734.52	210.60	139.29
30	275.76	1141.77	415.95	355.20
50	630.50	826.29	722.75	1002.36
100	2026.39	1879.08	802.93	1883.70

Table 12. Inertia for Scenery extend inference, higher is better

We attach a simple visualization of topics in scenery prompt generation, with topic n=100, cluster k=5.

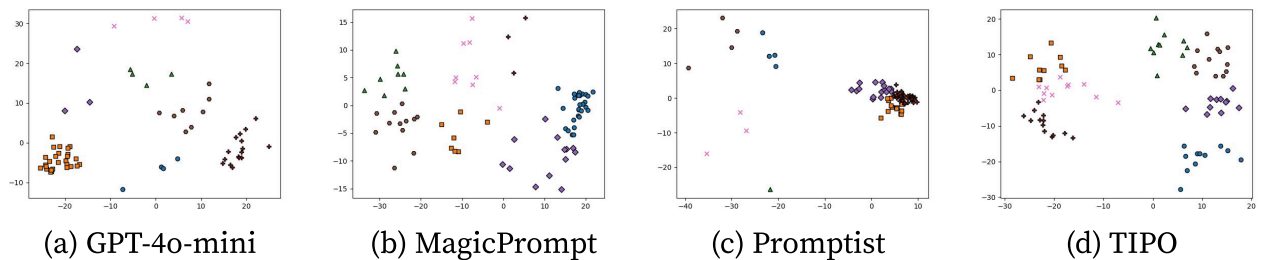


Figure 31. Topic visualization for scenery prompt generation. A wider spread indicates a greater diversity of generated topics.

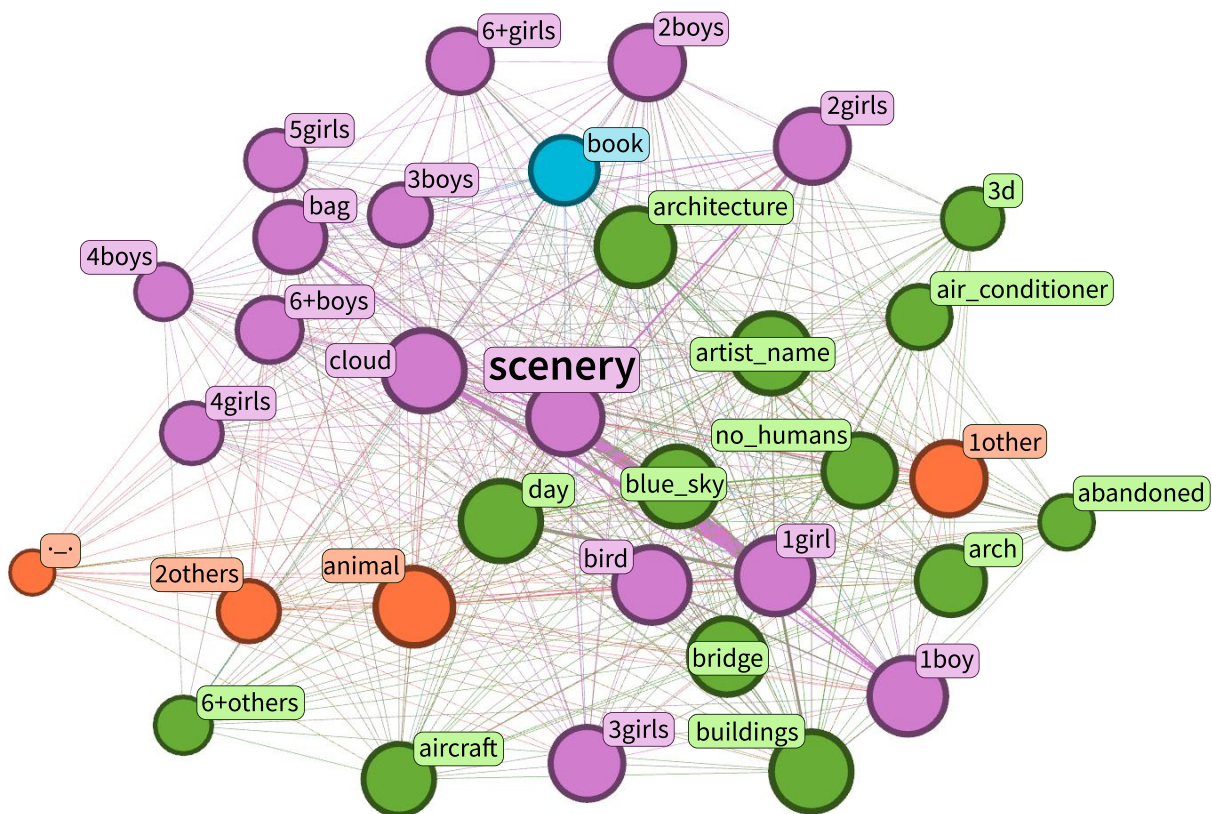


Figure 32. This visualization represents a filtered subset of posts from the Danbooru2023 dataset, centered on the 'scenery' tag. The network graph is an ego network (depth 1), which includes only nodes directly connected to the 'scenery' tag. To refine the data and focus on meaningful associations, uncommon tags with fewer than 10 occurrences were excluded. The analysis, conducted using Gephi, focuses on nodes with a degree greater than 600 to highlight critical components. Nodes are color-coded by modularity class by Fast Unfolding Algorithm [10], revealing clusters of closely associated tags. Node size reflects Eigenvector Centrality[11], emphasizing highly connected and influential tags within their network.

## I. Discussion and Future Work

Despite the promising performance demonstrated by TIPO, several areas merit further investigation:

**Personalization and User Adaptation.** TIPO currently does not directly incorporate personalization methods (e.g. LoRA [30]). Incorporating such modules could further align generated outputs to individual user preferences, enabling more tailored creative assistance. Investigating joint training strategies that integrate personalized fine-tuning represents a valuable future direction.

**Generalization to Uncommon Compositions.** While TIPO performs effectively on typical and broadly represented concepts, it may still struggle with highly unconventional combinations (e.g., “avocado chair”). Future research should systematically evaluate TIPO’s performance on rare or unusual prompts (but considered creative prompts), potentially exploring auxiliary training or adaptation methods to ensure broader compositional robustness.

**Capacity and Backbone Scalability.** Given TIPO model’s architecture [65, 66], its capacity for handling highly complex or lengthy prompts could be inherently limited. Future work could investigate more extensive or specialized architectures enhance compositional and semantic capacity, ideally without compromising real-time inference efficiency, are crucial for practical deployment.